

DESIGN OF DAMPING CONTROLLER FOR SVC

A DISSERTATION

Submitted in partial fulfillment of the
requirements for the award of the degree

of

MASTER OF TECHNOLOGY

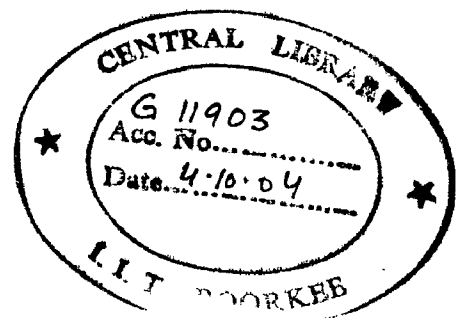
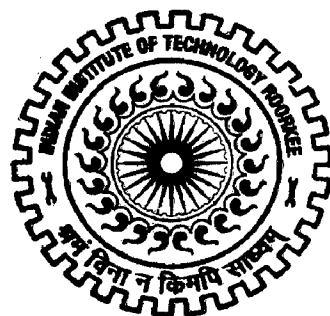
in

ELECTRICAL ENGINEERING

(With Specialization in Power System Engineering)

By

RAMPRASAD KUNTUMALLA



DEPARTMENT OF ELECTRICAL ENGINEERING
INDIAN INSTITUTE OF TECHNOLOGY ROORKEE
ROORKEE-247 667 (INDIA)
JUNE, 2004

CANDIDATE'S DECLARATION

This is to certify that the report which is being presented in this dissertation titled "Design of Damping Controller for SVC" in partial fulfillment of the requirements for the award of the degree of master of technology in electrical engineering, with specialization in power system engineering, submitted in the department of Electrical Engineering, Indian Institute of Technology, Roorkee is an authentic record of my own work under the supervision of Dr. Biswarup Das, Assist. Professor, Electrical Engineering Department, Indian Institute of Technology, Roorkee and Dr. Vinay Pant Assist. Professor, Electrical Engineering Department, Indian Institute of Technology, Roorkee.

The matter embodied in this report has not been submitted by me for the award of any other degree or diploma.

Place: Roorkee

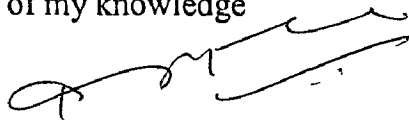
K. Ramprasad

Date:

(RAMPRASAD KUNTUMALLA)

CERTIFICATE

This is to certify that the above statement made by the student is correct to the best of my knowledge



(Dr. Vinay Pant)
Assistant professor
Dept. of Electrical Engineering
Indian Institute of Technology, Roorkee



(Dr. Biswarup Das)
Assistant professor
Dept. of Electrical Engineering
Indian Institute of Technology, Roorkee

ACKNOWLEDGEMENTS

I take this opportunity to express my deep sense of gratitude to both of my guides **Dr. B. Das**, Asst. Professor, Department of Electrical Engineering and **Dr. Vinay pant**, Asst. Professor, Department of Electrical Engineering, Indian Institute of Technology Roorkee, Roorkee for their continual guidance, constant encouragement, discussion and unceasing enthusiasm. I consider myself privileged to have worked under their guidance.

My heartfelt gratitude and indebtedness goes to **Dr. J.D.Sharma**, Professor of Electrical Engineering Department, **shri. Bharat gupta**, Asst. Professor of Electrical Engineering Department, **Dr. N.P.Padhy**, Asst. Professor of Electrical Engineering Department, who, with their encouraging and caring words, constructive criticism and suggestions, have contributed directly or indirectly in a significant way towards completion of this work.

My special Thanks goes to **Mr. Nandakishore**, Ph.D. scholar, AHEC Department Indian Institute of Technology Roorkee, Roorkee. I am thankful to **Mr. Dheeraj Kumar Kathode**, **Ms. Dhamanjeet Kour** and **Ashwani K. Chandel** for their valuable suggestions and comments.

I am highly grateful to **Shri S. K. Kapoor** and **Shri Jai Pal Singh**, Lab. Technicians, Power System Simulation Lab. for providing the required facilities and cooperation during this work.

Last but not the least; I thank all others who directly or indirectly helped me in my endeavor.

Ramprasad Kuntumalla

CONTENTS

CERTIFICATE	i
ACKNOWLEDGEMENT	ii
CONTENTS	iii
ABBREVIATIONS	v
ABSTRACT	vii
CHAPTER I: INTRODUCTION	1-4
1.1 Small Signal Stability problems	1
1.2 Literature review	2
CHAPTER II: MODELING OF SVC FOR LOAD FLOW STUDIES	5-9
2.1 Modeling of SVC for Load Flow studies	5
2.2 Flow chart for NRLF incorporating SVC	6
2.3 Comparison of voltage profile of the system	8
CHAPTER III: MODELLING OF MULTIMACHINE POWER SYSTEM AND SVC	10-24
3.1 Machine network transformation	10
3.2 DAE model of multi-machine power system	11
3.2.1 Differential equations for synchronous machine	12
3.2.2 Differential equation for exciter	12
3.2.3 Stator algebraic equations	12
3.2.4 Network equations	12
3.3 Block diagram of Dynamic model of SVC	21
3.4 Modification of linear model incorporating SVC	21
3.5 Computation of initial conditions	21
CHAPTER IV: LOCATION OF SVC AND SELECTION OF INPUT SIGNALS	24-31
4.1 Planning and preparing the system for the design of controller	25
4.2 Location of SVC for effective damping using modal analysis	26
4.3 Selection of input signal for the controller	28

CHAPTER V: DESIGN OF DAMPING CONTROLLER FOR SVC	32-39
5.1 Model order reduction	32
5.1.1 Objectives of model order reduction	32
5.1.2 Model order reduction of the system	34
5.1.3 The step response of higher order and reduced order systems	34
5.2 Design of damping controller	35
5.2.1 Objectives and constraints of damping controller	35
5.2.2 Components of damping controller	35
5.2.3 Method of design of damping controller	37
5.2.4 Tuning of damping controller	39
CHAPTER VI: RESULTS AND DISCUSSION	40-42
6.1 Results	40
6.2 Discussion	42
6.3 Conclusions	43

REFERENCES

APPENDIX A: 3 Machine 10 Bus system data for load flow and small signal stability analysis

APPENDIX B: Load flow results for the two different operating points

ABBREVIATIONS

- D-Q is network frame of reference
- d-q is machine frame of reference
- δ is rotor angle of synchronous machine
- ω_s is synchronous speed
- ω_i is rotor speed
- α_{ik} is the admittance angle between buses i and k
- M_i is inertia of the rotor
- E_{qi} is the internal voltage along q-axis
- E_{di} is the internal voltage along d-axis
- E_{fd} is the field excitation voltage on the rotor
- I_{qi} is the stator current along q-axis
- I_{di} is the stator current along d-axis
- ΔV_{ref} is the change in the reference voltage
- $\Delta V_{ref,SVC}$ is the change in the voltage reference value of the SVC
- ΔT_m is the change in the input mechanical torque
- V_i is the bus voltage
- θ_i is angle of voltage at the bus with respect to reference
- P_{Li} is the MW load at a bus
- Q_{Li} is the MVAR load at a bus
- R_s is the stator resistance
- X_d is the synchronous reactance along d-axis
- X_q is the synchronous reactance along q-axis
- X_d' is the transient synchronous reactance along d-axis
- X_q' is the transient synchronous reactance along d-axis
- K_A is the amplifier gain of static exciter
- T_A is the amplifier time constant of static exciter
- H is the rotor inertia in p.u.
- T_{do} is the time constant of the field along d-axis
- T_{qo} is the time constant of the field along q-axis

- D is the damping coefficient
- T_m is the measuring time constant of the transducer
- T_c is the controlling time constant of the SVC firing ckt.
- K_p is the proportional gain of the voltage regulator
- K_i is the integral time constant of the voltage regulator
- K is the slope of the SVC characteristics

ABSTRACT

In this work an attempt has been made to investigate the improvement of Small Signal Stability using SVC. For this purpose state space model for the 3 machine, 10 bus system is developed, in which a SVC has been installed in the middle of a transmission line. Reduced order model of the system is obtained for ease of analysis and design. Two operating conditions are considered, to show the robustness of the controller. To improve the damping of the system, a damping controller for SVC has been designed. The improvement in the system damping has been investigated by eigen value analysis and the results shows the effectiveness of the designed controller.

INTRODUCTION

1.1 SMALL SIGNAL STABILITY PROBLEMS [2]

“It is the ability of a power system to maintain synchronism, when subjected to small disturbances”. A disturbance is considered to be small if the equation describing the resulting response of the system may be linearized for the purpose of analysis.

Instability that may result can be of two forms:-

1. Steady increase in generator rotor angle due to lack of synchronizing torque.
2. Rotor oscillations of increasing size due to lack of sufficient damping torque.

In recent years in practical power systems the small signal stability problem is usually lack of sufficient damping of rotor oscillations.

Local problems

Local problems involve a small part of the system. They may be associated with rotor angle oscillations of a single generator or a single plant against the rest of the system. The stability problems related to such oscillations are similar to those of a single machine infinite bus system the most commonly encountered small signal stability problems are of this category this local problems also be associated with oscillation between rotors of a few generators close to each other. The local plant mode or inter plant mode oscillations have frequencies in the range of 0.7-2.0 Hz

Global problems

Global small signal stability problems are caused by interactions among large groups of generators and have wide spread effects. They involved oscillations of a group of generators in one area swinging against a group of generators in another area. Such oscillations are called inter area mode oscillations. Large interconnected systems usually have two distinct forms of inter areas oscillations.

- a) Very low frequency mode involving all the generators in the system. The system is essentially split into two parts with generators in one part swinging against machines in other part. The frequencies of oscillations of this mode are in the order of 0.1-0.3 Hz.
- b) High frequency mode involves sub groups of generators swinging against each other. The frequencies of oscillations of these modes are typically in the range of 0.4-0.7 Hz

1.2 LITERATURE REVIEW

The stability study of the system is predominantly dependent on the low frequency (0.1 - 2 Hz) rotor oscillation mode. A Power System Damping controller comprises of a lead/lag stage, a wash out stage and a high frequency filtering stage together with gain. The filter is designed to pass the swing mode frequency signal while allowing for any variation in the frequency range of system conditions. It rejects frequencies associated with non power swing modes, such as sub-synchronous torsional oscillation modes and modes relating to noise signals that over-ride the auxiliary control signals.

Gain-phase margin technique [1, 5, 37] has been applied for the design of damping controller. In this technique, the controller is designed primarily for dominant swing mode frequency. The amount of phase lead compensation required corresponding to pure damping condition is obtained. This phase angle is a function of the controllability and observability constraints. The damping controller will be designed and verified for different operating conditions.

Root Locus Technique [5,7,37] has been applied by various authors, in this work, For different auxiliary controllers, the loci of critical eigen values are obtained with varying controller parameters, each taken one at a time. Based on these root loci a range is selected for different parameters (K, T1 and T2) in which a high degree of stabilization is provided to the critical modes of the system. Power transfer limits are then evaluated for different combination of parameters in these ranges. The controller parameters which result in maximum power transfer are chosen as optimal for the particular auxiliary controller.

Damping Torque analysis [8] has been carried out mathematically for various input signals and it is shown that that the computed internal frequency (CIF) Provides maximum damping to the rotor mode at the considered operating point and results in the highest power transfer of all the signals investigated clearly indicating the importance of high observability of the mode to be damped in the auxiliary control signal. The synthesized signal CIF contains the effect of the swing mode in the highest measure and is thus effective.

Linear Quadratic Regulator (LQR) [9, 10] has been applied for the design of damping controller. The LQR technique is one of optimal control that can be used to co-ordinate the controllers. The control co-ordination method involves formulating an LQR problem to determine a full state feed-back controller in which a quadratic performance index is minimized. An output feedback controller is then obtained, based on the reduced eigen space of the full state solution. The dominant modes of the full state feed-back system are retained in the closed loop system with output feedback. Control is calculated through an algorithm on the basis of reduced order model of the power system. The control dampens the output of the system, reducing it to zero. The controller is a self tuning adaptive regulator.

For a controller based on linearized models, robust control theory [11, 12, 16, 17] has been applied. This technique explicitly considers the variations of the system operating condition using uncertainty models. The plant model under various operating conditions can be represented as the combination of uncertainty model and nominal model. A robust controller has been designed, so that the controller performance is satisfactory over a wide range of operating conditions.

Fuzzy logic control technique [13] has been used for damping controller. In this, variable gain is proposed to terminate the switching control of SVC soon after reaching quasi steady state to avoid excess and unnecessary control. Real power flow signal is used to determine the state of the system. Depending on the state and using simple Fuzzy Logic Control rules, the control is calculated which modifies the firing angles of SVC to give maximum system damping. Variable gain has to be exercised in quasi steady state, (i.e. the transition between capacitive and inductive period) for maximum damping.

The ANN stabilizing controller[14] scheme of the SVC consists of a neuro identifier and a neuro controller which has been developed based on a functional link network model. A recursive online training algorithm has been utilized to train the two networks. A neuro controller is developed to synthesize the control action being used as supplementary signal to the SVC. A neuro-identifier is used to identify the dynamics of the frequency deviation of the SVC regulating bus. The controller learning algorithm can provide such output by minimizing a quadratic cost function.

Damping controller has been designed using Genetic Algorithms [15], here, the optimization problem for robust, decentralized control may be restricted by problems of non-differentiability, non- linearity, and non-convexity. So for this, GA technique is used for the linearized state space model of the power system. The objective function is defined as the sum the damping ratios of all the modes of interest with constraints. This sum is evaluated over several likely operating conditions to introduce robustness. This optimization yields the gain K , and time constants T_1 and T_2 for all the controllers.

MODELING OF SVC FOR LOAD FLOW STUDIES

1.2.1 MODELING OF SVC FOR LOAD FLOW STUDIES [1, 18]

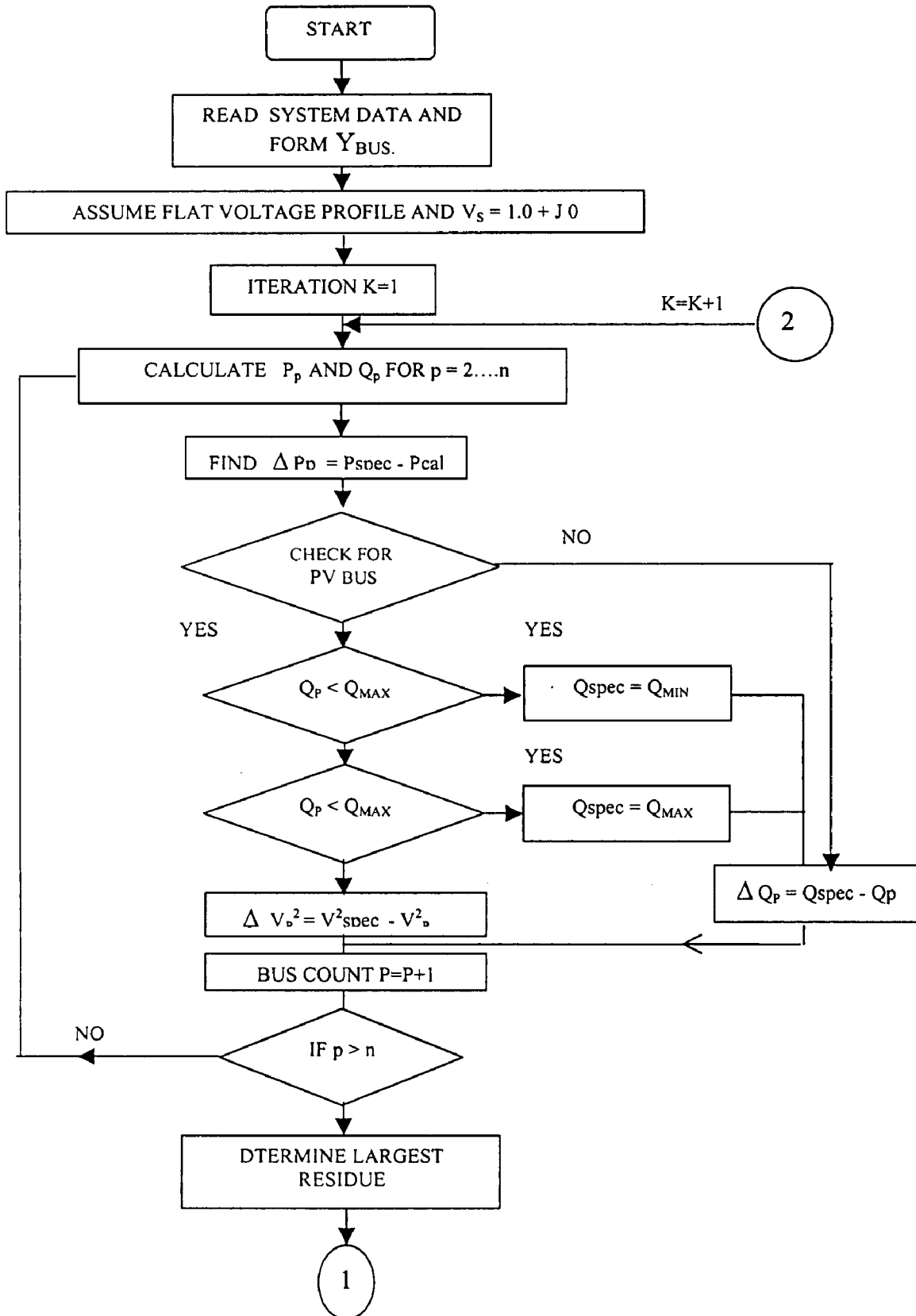
Load flow is a very important and powerful tool for power system analysis in planning stages. The models and load flow algorithms will mimic real time behavior of the system. So it is very important to consider the modeling of SVC for load flow analysis.

A simpler representation assumes that the SVC slope, accounting for voltage regulation is zero. This assumption may be acceptable as long as the SVC is operating within limits, but may lead to gross errors if the SVC is operating close to its reactive limits. Let us consider the upper limit of SVC, when the system is operating under low loading conditions. If the slope is taken to be zero, then the generator will violate its minimum reactive limit point $B_{xsl}=0$. However the generator will operate well within limits if the SVC slope is taken into account.

The SVC characteristic is represented by connecting the generator to a dummy bus coupled to the high voltage node via an inductive reactance whose value, on the SVC base, is equal to the per unit slope. The dummy bus is represented as a PV-type node whereas the high voltage node is represented as a PQ type node.

If the SVC operates outside the limits, the generator representation is no longer valid. In such cases, changing the SVC representation to a fixed reactive susceptance will yield accurate results. However both representations require a different number of nodes. The generator uses two or three nodes where as the fixed susceptance uses only one node. It takes the form of a variable susceptance when the SVC is operating within limits and it takes the form of a fixed susceptance otherwise.

2.2 FLOW CHART FOR NRLF INCORPORATING SVC



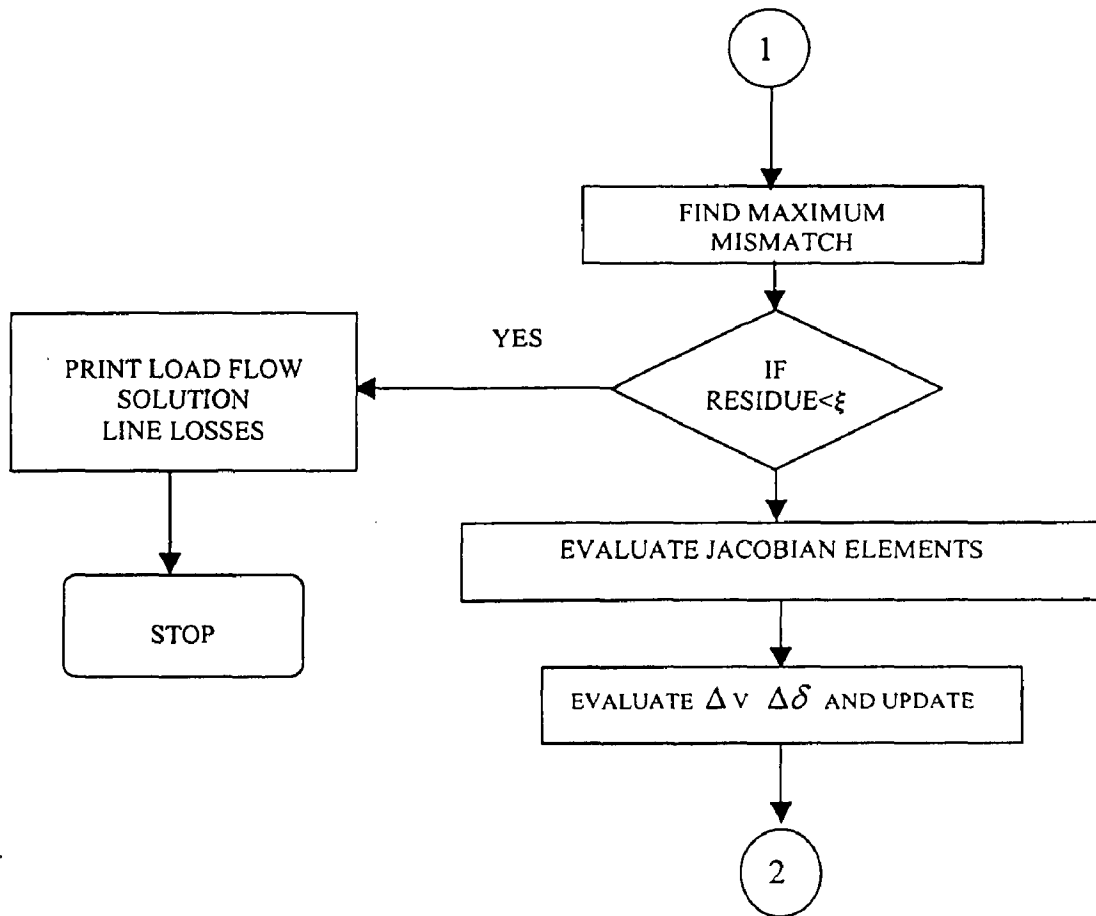


Figure 2.1: Flow chart for Newton Raphson Load Flow algorithm incorporating SVC

Figure 2.1 shows the flow chart of Newton Raphson Load Flow algorithm which is used in this work for obtaining load flow of the three machine ten bus system. The Load flow solutions of the system for two operating conditions are presented in APPENDIX B. The voltage profile of the system for both operating conditions is shown in the following next sections.

2.3 COMPARISON OF VOLTAGE PROFILE OF THE SYSTEM

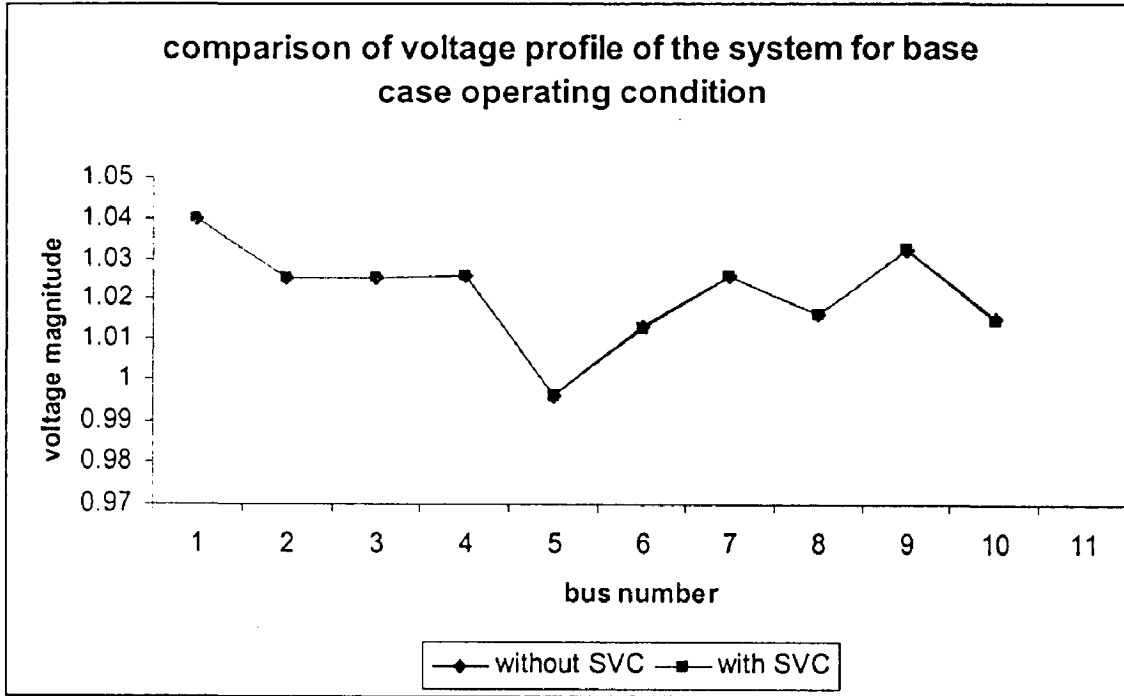


Figure 2.2 : comparison of voltage profile of the system for base case operating Condition with and without SVC

Figure 2.2 shows the voltage profile of the system for base case operating condition without SVC and with SVC are overlapped. The voltage boosted by the SVC is very less for this operating condition in steady state.

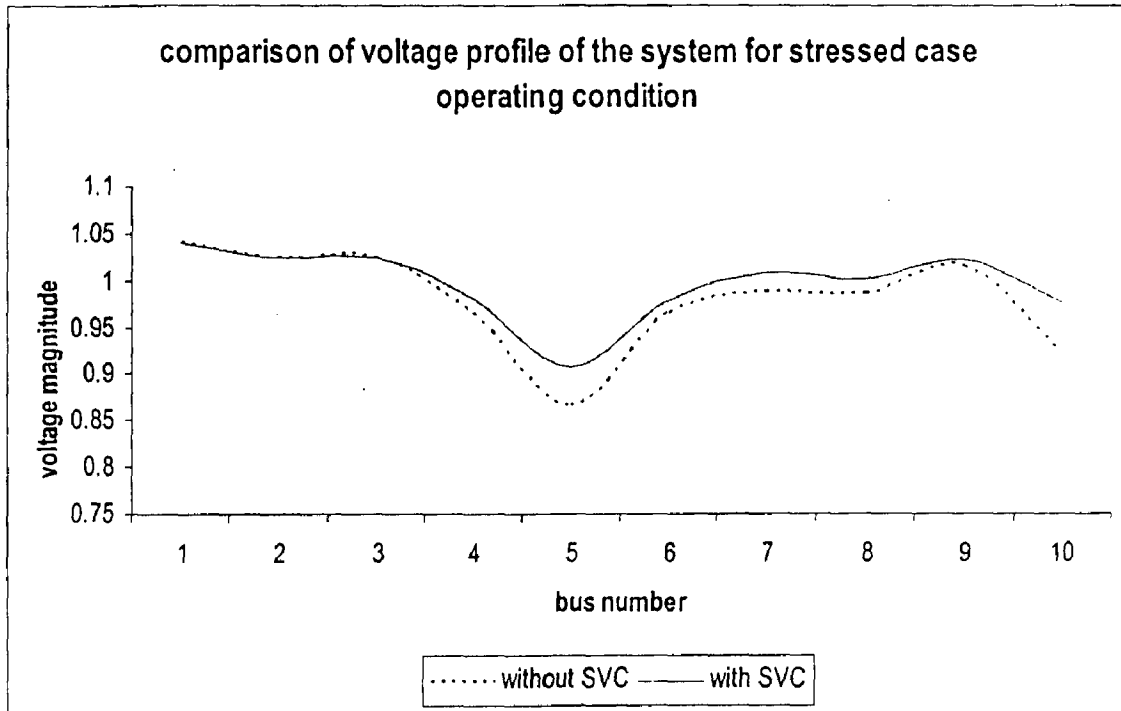


Figure 2.3 : Comparison of voltage profile of the system for stressed case operating condition with and without SVC

Figure 2.3 shows the voltage profile of the system for heavily stressed case operation near the point of collapse. There is a significant change in the voltage profile boosted up by the SVC in steady state.

The load flow solution obtained in this stage is used to initialize the dynamic stability program for the computation of initial conditions and eigen values are obtained thereafter.

MODELLING OF MULTI MACHINE POWER SYSTEM AND SVC

3.1 MACHINE NETWORK TRANSFORMATION [4, 20, 22, 30]

In this chapter we will consider the linearized differential algebraic equation (DAE) model of Multi Machine Power System. This is further linearized to form the system state equations. Following notations are used.

m = no. of generator buses (if there is infinite bus, it is machine no. 1)

n = total no. of buses in the system

b = total no. of branches in the system.

The machine network transformation is expressed as

$$\begin{bmatrix} F_{di} \\ F_{qi} \end{bmatrix} = \begin{bmatrix} \sin \delta_i & -\cos \delta_i \\ \cos \delta_i & \sin \delta_i \end{bmatrix} \begin{bmatrix} F_{Di} \\ F_{Qi} \end{bmatrix} \quad (3.1)$$

$$\begin{bmatrix} F_{Di} \\ F_{Qi} \end{bmatrix} = \begin{bmatrix} \sin \delta_i & \cos \delta_i \\ -\cos \delta_i & \sin \delta_i \end{bmatrix} \begin{bmatrix} F_{di} \\ F_{qi} \end{bmatrix} \quad (3.2)$$

for $i = 1 \dots m$

where F can either be voltage V or current I . Fig 3.1 shows the graphical representation of equations.

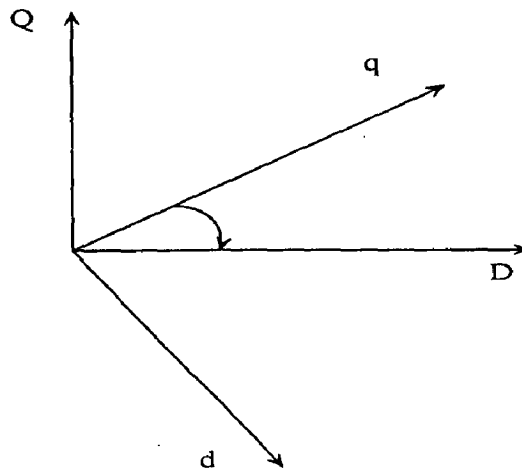


Figure 3.1 : Graphical representation of machine network transformation.

3.2 DAE MODEL FOR MULTI MACHINE POWER SYSTEM

This is a comprehensive dynamic model for study of low frequency oscillations in power system. Fig 3.1 shows the synchronous machine two axis model and fig 3.2 shows the static exciter model.

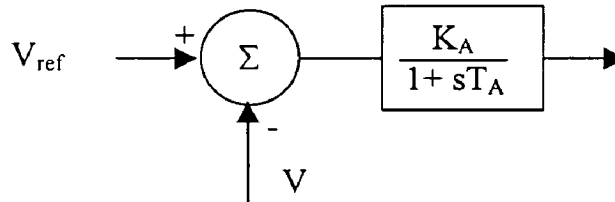


Figure 3.2 : Static exciter model

The assumptions for deriving this model are as follows

- 1) Stator has three coils in a balanced symmetrical configuration centered 120° electrical apart.
- 2) Rotor has four coils in a balanced symmetrical configuration located in pairs 90° electrical apart.
- 3) All energy stored in electrical system inside the machine terminals is included in the energy stored in coupling field.
- 4) The coupling field is lossless. This assumption neglects the phenomena such as hysteresis but not saturation.
- 5) The relationship between the flux linkages and currents must reflect a conservative coupling field. It must be independent of θ_{shaft} when expressed in d-q-o coordinate system.
- 6) Space harmonics are neglected.

3.2.1 Differential Equations for synchronous machine

$$\frac{d\delta}{dt} = \omega_i - \omega_s \quad (3.3)$$

$$\frac{d\omega}{dt} = \frac{T_i}{M_i} - \frac{[E'_{qi} - X'_{di} I_{di}] I_{qi}}{M_i} - \frac{[E'_{di} + X'_{qi} I_{qi}] I_{di}}{M_i} - \frac{D_i(\omega_i - \omega_s)}{M_i} \quad (3.4)$$

$$\frac{dE'_{di}}{dt} = \frac{E'_{di}}{T'_{qoi}} - \frac{(X_{qi} - X'_{qi}) I_{qi}}{T'_{qoi}} \quad (3.5)$$

$$\frac{dE'_{qi}}{dt} = \frac{E'_{qi}}{T'_{doi}} - \frac{(X_{di} - X'_{di}) I_{di}}{T'_{doi}} + \frac{E_{fdi}}{T'_{doi}} \quad (3.6)$$

3.2.2 Differential Equations for Exciter

$$\frac{dE_{fdi}}{dt} = -\frac{E_{fdi}}{T_{Ai}} + \frac{K_{Ai}}{T_{Ai}} (V_{ref} - V_i) \quad (3.7)$$

3.2.3 Stator algebraic equations

The stator algebraic equations in polar form are

$$E'_{di} - V_i \sin(\delta_i - \theta_i) - R_{si} I_{di} + X'_{qi} I_{qi} = 0 \quad (3.8)$$

$$E'_{qi} - V_i \cos(\delta_i - \theta_i) - R_{si} I_{qi} + X'_{di} I_{di} = 0 \quad (3.9)$$

3.2.4 Network equations are

the network equations are

$$I_{di} V_i \sin(\delta_i - \theta_i) + I_{qi} V_i \cos(\delta_i - \theta_i) + P_{Li}(V_i) - \sum_{k=1}^n V_k V_i Y_{ik} \cos(\delta_i - \theta_i - \alpha_{ik}) = 0 \quad (3.10)$$

$$I_{di} V_i \cos(\delta_i - \theta_i) - I_{qi} V_i \sin(\delta_i - \theta_i) + Q_{Li}(V_i) - \sum_{k=1}^n V_k V_i Y_{ik} \sin(\delta_i - \theta_i - \alpha_{ik}) = 0 \quad (3.11)$$

for $i=1, \dots, m$

$$P_{Li}(V_i) - \sum_{k=1}^n V_k V_i Y_{ik} \cos(\delta_i - \theta_i - \alpha_{ik}) = 0 \quad (3.12)$$

$$Q_{Li}(V_i) - \sum_{k=1}^n V_k V_i Y_{ik} \sin(\delta_i - \theta_i - \alpha_{ik}) = 0 \quad (3.13)$$

for $i=m+1, \dots, n$

(3.14)

The linearization of the differential equations yields

$$\frac{d\Delta\delta}{dt} = \Delta\varpi_i$$

(3.15)

$$\begin{aligned} \frac{d\Delta\varpi}{dt} = & \frac{\Delta T_i}{M_i} - \frac{[E'_{qi} - X'_{di} I_{di}] \Delta I_{qi}}{M_i} + \frac{[-\Delta E'_{qi} + X'_{di} \Delta I_{di}] I_{qi}}{M_i} - \frac{[E'_{di} + X'_{qi} I_{qi}] \Delta I_{di}}{M_i} \\ & - \frac{[\Delta E'_{di} + X'_{qi} \Delta I_{qi}] I_{di}}{M_i} - \frac{D_i(\Delta\varpi_i)}{M_i} \end{aligned}$$

(3.16)

$$\frac{d\Delta E'_{di}}{dt} = \frac{\Delta E'_{di}}{T'_{qoi}} - \frac{(X_{qi} - X'_{qi}) \Delta I_{qi}}{T'_{qoi}}$$

(3.17)

$$\frac{d\Delta E'_{qi}}{dt} = -\frac{\Delta E'_{qi}}{T'_{doi}} - \frac{(X_{di} - X'_{di}) \Delta I_{di}}{T'_{doi}} + \frac{\Delta E_{fdi}}{T'_{doi}}$$

(3.18)

$$\frac{d\Delta E_{fdi}}{dt} = -\frac{1}{T'_{Ai}} \Delta E_{fdi} + \frac{K_{Ai}}{T'_{Ai}} (\Delta V_{ref} - \Delta V_i)$$

where the symbol ∂ stands for partial derivative.

Writing (3.14)-(3.18) in matrix form we obtain,

$$\begin{bmatrix} \Delta \delta \\ \Delta \varpi \\ \Delta E_{qi} \\ \Delta E_{di} \\ \Delta E_{fdi} \end{bmatrix} = \begin{bmatrix} 0 & 1 & 0 & 0 & 0 \\ 0 & \frac{-D_i}{M_i} & \frac{-I_{qio}}{M_i} & \frac{-I_{dio}}{M_i} & 0 \\ 0 & 0 & \frac{-1}{T'_{dio}} & 0 & \frac{1}{T'_{dio}} \\ 0 & 0 & 0 & \frac{-1}{T'_{qio}} & 0 \\ 0 & 0 & 0 & 0 & \frac{-1}{T_{Ai}} \end{bmatrix} \begin{bmatrix} \Delta \delta \\ \Delta \varpi \\ \Delta E_{qi} \\ \Delta E_{di} \\ \Delta E_{fdi} \end{bmatrix}$$

$$+ \begin{bmatrix} 0 & 0 \\ \frac{I_{qio}(X'_{di} - X'_{qi}) - E'_{dio}}{M_i} & \frac{I_{dio}(X'_{di} - X'_{qi}) - E'_{qio}}{M_i} \\ -\frac{(X_{di} - X'_{di})}{T'_{doi}} & 0 \\ 0 & \frac{X_{qi} - X'_{qi}}{T'_{qio}} \\ 0 & 0 \end{bmatrix} \begin{bmatrix} \Delta I_{di} \\ \Delta I_{qi} \end{bmatrix}$$

$$+ \begin{bmatrix} 0 & 0 \\ 0 & 0 \\ 0 & 0 \\ 0 & 0 \\ 0 & -\frac{K_{Ai}}{T_{Ai}} \end{bmatrix} \begin{bmatrix} \Delta \theta_i \\ \Delta V_i \end{bmatrix} + \begin{bmatrix} 0 & 0 \\ \frac{1}{M_i} & 0 \\ 0 & 0 \\ 0 & 0 \\ 0 & \frac{K_{Ai}}{T_{Ai}} \end{bmatrix} \begin{bmatrix} \Delta T_{Mi} \\ \Delta V_{r/i} \end{bmatrix} \text{ for } i = 1, \dots, m \quad (3.19)$$

In simplified form.

$$\begin{bmatrix} \Delta x_i \end{bmatrix} = [A_{Li}] [\Delta x_i] + [B_{li}] [\Delta I_{gi}] + [B_{2i}] [\Delta V_{gi}] + [E_i] [\Delta u_i] \quad \text{for } i=1, \dots, m \quad (3.20)$$

$$\text{where } [\Delta I_{gi}] = \begin{bmatrix} \Delta I_{di} \\ \Delta I_{qi} \end{bmatrix}, [\Delta V_{gi}] = \begin{bmatrix} \Delta \theta_i \\ \Delta V_i \end{bmatrix}, \text{ and } [\Delta u_i] = \begin{bmatrix} \Delta T_{Mi} \\ \Delta V_{refl} \end{bmatrix} \quad (3.21)$$

for 'm' machine system above equation can be expressed in matrix form as,

$$\begin{bmatrix} \Delta x \end{bmatrix} = [A_i] [\Delta x] + [B_i] [\Delta I_g] + [B_2] [\Delta V_g] + [E_i] [\Delta U] \quad (3.22)$$

where, $[A_i]$, $[B_i]$, $[B_2]$ and $[E_i]$ are block diagonal matrices.

Now linearizing the stator algebraic equation (3.8)-(3.9) we get,

$$\begin{aligned} \Delta E'_{di} - \sin(\delta_{io} - \theta_{io}) \Delta V_i - V_{io} \cos(\delta_{io} - \theta_{io}) \Delta \delta_i + V_{io} \cos(\delta_{io} - \theta_{io}) \Delta \theta_i \\ - R_{si} \Delta I_{di} + X'_{qi} \Delta I_{qi} = 0 \end{aligned} \quad (3.23)$$

$$\begin{aligned} \Delta E'_{qi} - \cos(\delta_{io} - \theta_{io}) \Delta V_i + V_{io} \sin(\delta_{io} - \theta_{io}) \Delta \delta_i - V_{io} \sin(\delta_{io} - \theta_{io}) \Delta \theta_i \\ - R_{si} \Delta I_{qi} + X'_{di} \Delta I_{di} = 0 \quad i = 1, \dots, m \end{aligned} \quad (3.24)$$

Writing equation (3.23)-(3.24) in matrix form, we have,

$$\begin{bmatrix} -V_{io} \cos(\delta_{io} - \theta_{io}) & 0 & 0 & 1 & 0 \\ V_{io} \sin(\delta_{io} - \theta_{io}) & 0 & 1 & 1 & 0 \end{bmatrix} \begin{bmatrix} \Delta \delta_i \\ \Delta \omega_i \\ \Delta E'_{qi} \\ \Delta E'_{di} \\ \Delta E'_{fdi} \end{bmatrix} + \begin{bmatrix} -R_{si} & X'_{qi} \\ -X'_{di} & -R_{si} \end{bmatrix} \begin{bmatrix} \Delta I_{di} \\ \Delta I_{qi} \end{bmatrix} + \begin{bmatrix} V_{io} \cos(\delta_{io} - \theta_{io}) - \sin(\delta_{io} - \theta_{io}) \\ -V_{io} \sin(\delta_{io} - \theta_{io}) - \cos(\delta_{io} - \theta_{io}) \end{bmatrix} \begin{bmatrix} \Delta \theta_i \\ \Delta V_i \end{bmatrix} = 0 \quad i = 1, \dots, m \quad (3.25)$$

Rewriting above equation we obtain,

$$0 = [C_{li}] [\Delta x_i] + [D_{li}] [\Delta I_{gi}] + [D_{2i}] [\Delta V_{gi}] \quad i = 1, \dots, m \quad (3.26)$$

In matrix notation,

$$0 = [C_i][\Delta x] + [D_1][\Delta I_g] + [D_2][\Delta V_g] \quad i = 1 \dots m \quad (3.27)$$

where $[C_i]$, $[D_1]$ and $[D_2]$ are block diagonal matrices.

Linearizing the network equation (3.10)-(3.11), which pertain to generators, we obtain.

$$\begin{aligned} & V_{io} \sin(\delta_{io} - \theta_{io}) \Delta I_{di} + I_{dio} \sin(\delta_{io} - \theta_{io}) \Delta V_i + I_{dio} V_{io} \cos(\delta_{io} - \theta_{io}) \Delta \delta_i \\ & - I_{dio} V_{io} \cos(\delta_{io} - \theta_{io}) \Delta \theta_i + V_{io} \cos(\delta_{io} - \theta_{io}) \Delta I_{qi} \\ & + I_{qio} \cos(\delta_{io} - \theta_{io}) \Delta V_i - I_{qio} V_{io} \sin(\delta_{io} - \theta_{io}) \Delta \delta_i \\ & + I_{qio} V_{io} \sin(\delta_{io} - \theta_{io}) \Delta \theta_i - \left[\sum_{k=1}^n V_{ko} Y_{ik} \cos(\theta_{io} - \theta_{ko} - \alpha_{ik}) \right] \Delta V_i \\ & - V_{io} \sum_{\substack{k=1 \\ \neq i}}^n [Y_{ik} \cos(\theta_{io} - \theta_{ko} - \alpha_{ik})] \Delta V_k + \left[V_{io} \sum_{\substack{k=1 \\ \neq i}}^n V_{ko} Y_{ik} \sin(\theta_{io} - \theta_{ko} - \alpha_{ik}) \right] \Delta \theta_i \\ & - V_{io} \sum_{\substack{k=1 \\ \neq i}}^n [V_{ko} Y_{ik} \sin(\theta_{io} - \theta_{ko} - \alpha_{ik})] \Delta \theta_k + \frac{\partial P_{Li}(V_i)}{\partial V_i} \Delta V_i = 0 \end{aligned} \quad (3.28)$$

$$\begin{aligned} & V_{io} \cos(\delta_{io} - \theta_{io}) \Delta I_{di} + I_{dio} \cos(\delta_{io} - \theta_{io}) \Delta V_i - I_{dio} V_{io} \sin(\delta_{io} - \theta_{io}) \Delta \delta_i \\ & + I_{dio} V_{io} \sin(\delta_{io} - \theta_{io}) \Delta \theta_i - V_{io} \sin(\delta_{io} - \theta_{io}) \Delta I_{qi} \\ & - I_{qio} \sin(\delta_{io} - \theta_{io}) \Delta V_i - I_{qio} V_{io} \cos(\delta_{io} - \theta_{io}) \Delta \delta_i \\ & + I_{qio} V_{io} \cos(\delta_{io} - \theta_{io}) \Delta \theta_i - \left[\sum_{k=1}^n V_{ko} Y_{ik} \sin(\theta_{io} - \theta_{ko} - \alpha_{ik}) \right] \Delta V_i \\ & - V_{io} \sum_{\substack{k=1 \\ \neq i}}^n [Y_{ik} \sin(\theta_{io} - \theta_{ko} - \alpha_{ik})] \Delta V_k - \left[V_{io} \sum_{\substack{k=1 \\ \neq i}}^n V_{ko} Y_{ik} \cos(\theta_{io} - \theta_{ko} - \alpha_{ik}) \right] \Delta \theta_i \\ & + V_{io} \sum_{\substack{k=1 \\ \neq i}}^n [V_{ko} Y_{ik} \cos(\theta_{io} - \theta_{ko} - \alpha_{ik})] \Delta \theta_k + \frac{\partial Q_{Li}(V_i)}{\partial V_i} \Delta V_i = 0 \\ & i = 1, \dots, m \end{aligned} \quad (3.29)$$

Rewriting the above equations in matrix form we get,

$$0 = \begin{bmatrix} C_{21} & & \\ & \ddots & \\ & & C_{2m} \end{bmatrix} \begin{bmatrix} \Delta x_l \\ \vdots \\ \Delta x_m \end{bmatrix} + \begin{bmatrix} D_{32} & & \\ & \ddots & \\ & & D_{3m} \end{bmatrix} \begin{bmatrix} \Delta I_{gi} \\ \vdots \\ \Delta I_{gm} \end{bmatrix} \quad (3.30)$$

$$\begin{bmatrix} D_{41,1} & \cdots & D_{41,m} \\ \vdots & \vdots & \vdots \\ D_{4m,1} & \cdots & D_{4m,m} \end{bmatrix} \begin{bmatrix} \Delta V_{gl} \\ \vdots \\ \Delta V_{gm} \end{bmatrix} + \begin{bmatrix} D_{51,m+1} & \cdots & D_{51,n} \\ \vdots & \vdots & \vdots \\ D_{5m,m+1} & \cdots & D_{5m,n} \end{bmatrix} \begin{bmatrix} \Delta V_{lm+1} \\ \vdots \\ \Delta V_{ln} \end{bmatrix}$$

Where the various sub matrices are as follows:

$$C_{2i} = \begin{bmatrix} I_{dio} V_{io} \cos(\delta_{io} - \theta_{io}) - I_{qio} V_{io} \sin(\delta_{io} - \theta_{io}) & 0 & 0 & 0 & 0 & 0 & 0 \\ -I_{dio} V_{io} \sin(\delta_{io} - \theta_{io}) - I_{qio} V_{io} \cos(\delta_{io} - \theta_{io}) & 0 & 0 & 0 & 0 & 0 & 0 \end{bmatrix} \quad (3.31)$$

$$D_{3i} = \begin{bmatrix} V_{io} \sin(\delta_{io} - \theta_{io}) & V_{io} \cos(\delta_{io} - \theta_{io}) \\ V_{io} \cos(\delta_{io} - \theta_{io}) & -V_{io} \sin(\delta_{io} - \theta_{io}) \end{bmatrix}$$

$$D_{4i,i} = \begin{bmatrix} I_{dio} V_{io} \cos(\delta_{io} - \theta_{io}) - I_{qio} V_{io} \sin(\delta_{io} - \theta_{io}) & I_{dio} \sin(\delta_{io} - \theta_{io}) + I_{qio} \cos(\delta_{io} - \theta_{io}) \\ + V_{io} \sum_{\substack{k=1 \\ \neq i}}^n V_{ko} Y_{ik} \sin(\theta_{io} - \theta_{ko} - \alpha_{ik}) & - \sum_{k=1}^n V_{ko} Y_{ik} \cos(\theta_{io} - \theta_{ko} - \alpha_{ik}) \\ & - V_{io} Y_{ii} \cos(\alpha_{ii}) + \frac{\partial P_{Li}(V_i)}{\partial V_i} \\ I_{dio} V_{io} \sin(\delta_{io} - \theta_{io}) + I_{qio} V_{io} \cos(\delta_{io} - \theta_{io}) & I_{dio} \cos(\delta_{io} - \theta_{io}) - I_{qio} \sin(\delta_{io} - \theta_{io}) \\ - V_{io} \sum_{\substack{k=1 \\ \neq i}}^n V_{ko} Y_{ik} \cos(\theta_{io} - \theta_{ko} - \alpha_{ik}) - \sum_{k=1}^n V_{ko} Y_{ik} \sin(\theta_{io} - \theta_{ko} - \alpha_{ik}) & \\ & + \frac{\partial Q_{Li}(V_i)}{\partial V_i} \end{bmatrix} \begin{bmatrix} \Delta \theta_i \\ \vdots \\ \Delta V_i \end{bmatrix}$$

$i = 1, \dots, m$

(3.32)

$$D_{4i,k} = \begin{bmatrix} -V_{io} V_{ko} Y_{ik} \sin(\theta_{io} - \theta_{ko} - \alpha_{ik}) - V_{io} Y_{ik} \cos(\theta_{io} - \theta_{ko} - \alpha_{ik}) \\ V_{io} V_{ko} Y_{ik} \cos(\theta_{io} - \theta_{ko} - \alpha_{ik}) - V_{io} Y_{ik} \sin(\theta_{io} - \theta_{ko} - \alpha_{ik}) \end{bmatrix} \begin{matrix} i = 1, \dots, m \\ k = 1, \dots, m \end{matrix} \quad (3.33)$$

$$D_{5i,k} = \begin{bmatrix} -V_{io} V_{ko} Y_{ik} \sin(\theta_{io} - \theta_{ko} - \alpha_{ik}) - V_{io} Y_{ik} \cos(\theta_{io} - \theta_{ko} - \alpha_{ik}) \\ V_{io} V_{ko} Y_{ik} \cos(\theta_{io} - \theta_{ko} - \alpha_{ik}) - V_{io} Y_{ik} \sin(\theta_{io} - \theta_{ko} - \alpha_{ik}) \end{bmatrix} \begin{matrix} i = 1, \dots, m \\ k = m+1, \dots, n \end{matrix} \quad (3.34)$$

In matrix notation.

$$0 = [C_2][\Delta x] + [D_3][\Delta I_g] + [D_4][\Delta V_g] + [D_5][\Delta V_l] \quad (3.35)$$

where
$$\Delta V_{li} = \begin{bmatrix} \Delta \theta_i \\ \Delta V_i \end{bmatrix}$$

Here $[C_2]$ and $[D_3]$ are block diagonal matrices, whereas $[D_4]$, $[D_5]$ are full matrices.

Linearizing the network equations (3.12)-(3.13) for load buses, we obtain.

$$0 = \frac{\partial P_{Li}(V_i)}{\partial V_i} \Delta V_i - \left[\sum_{k=1}^n V_{ko} Y_{ik} \cos(\theta_{io} - \theta_{ko} - \alpha_{ik}) \right] \Delta V_i + \left[\sum_{\substack{k=1 \\ \neq i}}^n V_{io} V_{ko} Y_{ik} \sin(\theta_{io} - \theta_{ko} - \alpha_{ik}) \right] \Delta \theta_i \\ - V_{io} \sum_{k=1}^n [Y_{ik} \cos(\theta_{io} - \theta_{ko} - \alpha_{ik})] \Delta V_k - V_{io} \sum_{\substack{k=1 \\ \neq i}}^n [V_{ko} Y_{ik} \sin(\theta_{io} - \theta_{ko} - \alpha_{ik})] \Delta \theta_k \quad (3.36)$$

$$0 = \frac{\partial Q_{Li}(V_i)}{\partial V_i} \Delta V_i - \left[\sum_{k=1}^n V_{ko} Y_{ik} \sin(\theta_{io} - \theta_{ko} - \alpha_{ik}) \right] \Delta V_i - \left[\sum_{\substack{k=1 \\ \neq i}}^n V_{io} V_{ko} Y_{ik} \cos(\theta_{io} - \theta_{ko} - \alpha_{ik}) \right] \Delta \theta_i \\ - V_{io} \sum_{k=1}^n [Y_{ik} \sin(\theta_{io} - \theta_{ko} - \alpha_{ik})] \Delta V_k + V_{io} \sum_{\substack{k=1 \\ \neq i}}^n [V_{ko} Y_{ik} \cos(\theta_{io} - \theta_{ko} - \alpha_{ik})] \Delta \theta_k \\ i = m+1, \dots, n \quad (3.37)$$

Rewriting in matrix form we get,

$$0 = \begin{bmatrix} D_{6m+1,1} & \cdots & D_{6m+1,m} \\ \vdots & \vdots & \vdots \\ D_{6n,1} & \cdots & D_{6n,m} \end{bmatrix} \begin{bmatrix} \Delta V_{g1} \\ \vdots \\ \Delta V_{gm} \end{bmatrix} + \begin{bmatrix} D_{7m+1,m+1} & \cdots & D_{7m+1,n} \\ \vdots & \vdots & \vdots \\ D_{7n,m+1} & \cdots & D_{7n,n} \end{bmatrix} \begin{bmatrix} \Delta V_{lm+1} \\ \vdots \\ \Delta V_{ln} \end{bmatrix} \quad (3.38)$$

The various sub matrices are defined as follows:

$$D_{6i,k} = \begin{bmatrix} -V_{io} V_{ko} Y_{ik} \sin(\theta_{io} - \theta_{ko} - \alpha_{ik}) - V_{io} Y_{ik} \cos(\theta_{io} - \theta_{ko} - \alpha_{ik}) \\ V_{io} V_{ko} Y_{ik} \cos(\theta_{io} - \theta_{ko} - \alpha_{ik}) - V_{io} Y_{ik} \sin(\theta_{io} - \theta_{ko} - \alpha_{ik}) \end{bmatrix} \\ i = m+1, \dots, n \\ k = 1, \dots, n \quad (3.39)$$

$$D_{7i,i} = \left[\begin{array}{l} \sum_{k=1}^n V_{io} V_{ko} Y_{ik} \sin(\theta_{io} - \theta_{ko} - \alpha_{ik}) \frac{\partial P_{Li}(V_i)}{\partial V_i} - \sum_{k=1}^n \frac{V_{ko} Y_{ik} \cos(\theta_{io} - \theta_{ko} - \alpha_{ik})}{-V_{io} Y_{ik} \cos(\alpha_{ik})} \\ - \sum_{k=1}^n V_{io} V_{ko} Y_{ik} \cos(\theta_{io} - \theta_{ko} - \alpha_{ik}) \frac{\partial Q_{Li}(V_i)}{\partial V_i} - \sum_{k=1}^n \frac{V_{ko} Y_{ik} \sin(\theta_{io} - \theta_{ko} - \alpha_{ik})}{-V_{io} Y_{ik} \sin(\alpha_{ik})} \end{array} \right] \quad (3.40)$$

$i = m+1, \dots, n$

$$D_{7i,k} = \left[\begin{array}{l} -V_{io} V_{ko} Y_{ik} \sin(\theta_{io} - \theta_{ko} - \alpha_{ik}) - V_{io} Y_{ik} \cos(\theta_{io} - \theta_{ko} - \alpha_{ik}) \\ V_{io} V_{ko} Y_{ik} \cos(\theta_{io} - \theta_{ko} - \alpha_{ik}) - V_{io} Y_{ik} \sin(\theta_{io} - \theta_{ko} - \alpha_{ik}) \end{array} \right] \quad (3.41)$$

$i = m+1, \dots, n$
 $k = m+1, \dots, n$

Rewriting in compact form we obtain,

$$0 = [D_6] [\Delta V_g] + [D_7] [\Delta V_l] \quad (3.42)$$

where $[D_6]$ and $[D_7]$ are full matrices.

Rewriting the above equations together we have,

$$[\Delta \dot{x}] = [A_1] [\Delta x] + [B_1] [\Delta I_g] + [B_2] [\Delta V_g] + [E_1] [\Delta U] \quad (3.43)$$

$$0 = [C_1] [\Delta \dot{x}] + [D_1] [\Delta I_g] + [D_2] [\Delta V_g] \quad (3.44)$$

$$0 = [C_2] [\Delta x] + [D_3] [\Delta I_g] + [D_4] [\Delta V_g] + [D_5] [\Delta V_l] \quad (3.45)$$

$$0 = [D_6] [\Delta V_g] + [D_7] [\Delta V_l] \quad (3.46)$$

Eliminating ΔI_g and writing in matrix for, we obtain,

$$\begin{bmatrix} \Delta \dot{x} \\ 0 \end{bmatrix} = \begin{bmatrix} A' & B' \\ C' & D' \end{bmatrix} \begin{bmatrix} \Delta x \\ \Delta V_n \end{bmatrix} + \begin{bmatrix} E_1 \\ 0 \end{bmatrix} \Delta u \quad (3.47)$$

$$\text{where } A' = [A_1] - [B_1] [D_1^{-1}] [C_1] \quad (3.48)$$

$$B' = [B_2] - [B_1] [D_1^{-1}] [D_2] \quad (3.49)$$

$$C' = [C_2] - [D_3] [D_1^{-1}] [C_1] \quad (3.50)$$

$$D' = \begin{bmatrix} [D_4] - [D_3][D_1^{-1}][D_2][D_5] & \\ & [D_6] & [D_7] \end{bmatrix} \quad (3.51)$$

$$\Delta V_N = \begin{bmatrix} \Delta V_g \\ \Delta V_1 \end{bmatrix} \quad (3.52)$$

Reordering the variables in voltage vector, we get,

$$\Delta V_p = [\Delta y_c'] [\Delta y_b'] = [\Delta \theta_1 \Delta V_1 \dots \Delta V_m | \Delta \theta_2 \dots \Delta \theta_n \Delta V_{m+1} \dots \Delta V_n]' \quad (3.53)$$

After reordering equation (3.47) as in equation (3.53)

$$\begin{bmatrix} \Delta \dot{x} \\ 0 \\ 0 \end{bmatrix} = \begin{bmatrix} A' & B_1' & B_2' \\ C_1' & D_{11}' & D_{12}' \\ C_2' & D_{21}' & D_{22}' \end{bmatrix} \begin{bmatrix} \Delta x \\ \Delta y_c \\ \Delta y_b \end{bmatrix} + \begin{bmatrix} E_1 \\ 0 \\ 0 \end{bmatrix} \Delta u \quad (3.54)$$

where Δy_b is the set of load flow variables, and Δy_c is the set of other algebraic variables in the network equations. The system state equation is finally as follows.

$$[\Delta \dot{x}] = [A_{sys}] [\Delta x] + [E] [\Delta u] \quad (3.55)$$

where

$$[A_{sys}] = [A'] - \begin{bmatrix} B_1' \\ B_2' \end{bmatrix} [J'_{AE}]^{-1} \begin{bmatrix} C_1' \\ C_2' \end{bmatrix} \quad \text{where } J'_{AE} = \begin{bmatrix} D_{11}' & D_{12}' \\ D_{21}' & D_{22}' \end{bmatrix} \quad (3.56)$$

Eigenvalues of Matrix A_{sys} are computed to predict the stability of the system.

3.3 BLOCK DIAGRAM OF DYNAMIC MODEL OF THE SVC [19, 21, 23]

Dynamic model of SVC for dynamic stability analysis is given as

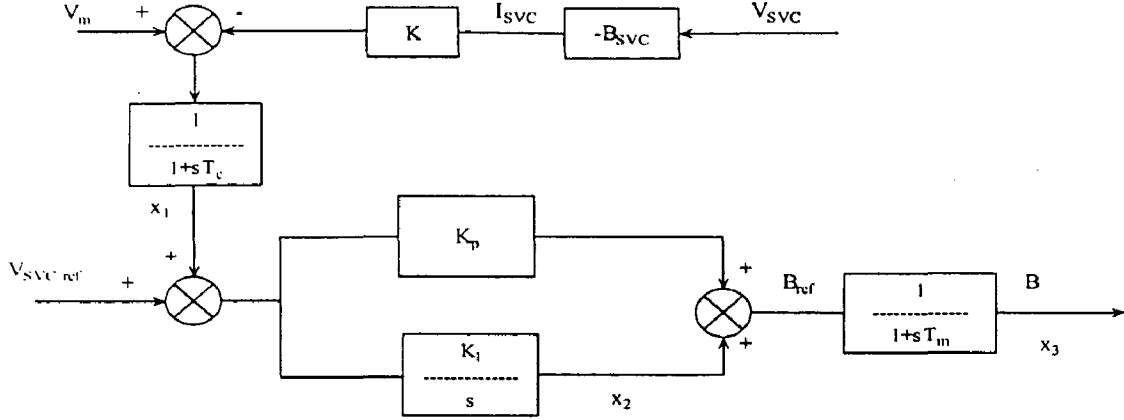


Figure 3.1 : SVC block diagram

3.4 MODIFICATION OF LINEAR MODEL INCORPORATING SVC

Here the admittance of the SVC seen by the system, B_{svc} , is the state variable x_3 . The block K is the slope of the control characteristic. Here $K_p=0$, so that integrator voltage regulator is used. The SVC block diagram model I shown in figure3.1. The state equations of the SVC are

$$\dot{x}_1 = \frac{1}{T_M} (V_{svc} (1 + Kx_3) - x_1) \quad (3.57)$$

$$\dot{x}_2 = Ki(V_{ref,svc} - x_1) \quad (3.58)$$

$$\dot{x}_3 = \frac{1}{T_c} (x_2 + K_p (V_{ref,svc} - x_1) - x_3) \quad (3.59)$$

$$Q_{svc} = -(V_{svc}^2 x_3) \quad (3.60)$$

When these equations are linearized

$$\Delta \dot{x}_1 = \frac{1}{T_M} (\Delta V_{svc} (1 + Kx_3) + V_{svc} K \Delta x_3 - \Delta x_1) \quad (3.61)$$

$$\Delta \dot{x}_2 = Ki(\Delta V_{ref,svc} - \Delta x_1) \quad (3.62)$$

$$\Delta \dot{x}_3 = \frac{1}{T_c} (\Delta x_2 + K_p (\Delta V_{ref,svc} - \Delta x_1) - \Delta x_3) \quad (3.63)$$

$$\Delta Q_{svc} = -(V_{svc}^2 \Delta x_3 + 2V_{svc} x_3 \Delta V_{svc}) \quad (3.64)$$

Arranging in matrix form we obtain

$$\begin{bmatrix} \Delta \dot{x}_1 \\ \Delta \dot{x}_2 \\ \Delta \dot{x}_3 \end{bmatrix} = \begin{bmatrix} \frac{-1}{T_M} & 0 & \frac{KV_{SVC}}{T_M} \\ -KI & 0 & 0 \\ \frac{-Kp}{T_c} & \frac{-1}{T_c} & \frac{-1}{T_c} \end{bmatrix} \begin{bmatrix} \Delta x_1 \\ \Delta x_2 \\ \Delta x_3 \end{bmatrix} + \begin{bmatrix} \frac{1+Kx_3}{T_M} \\ 0 \\ 0 \end{bmatrix} [\Delta V_{SVC}] \quad (3.65)$$

where

$$\Delta \dot{x}_{SVC} = A_{SVC} \Delta x_{SVC} + B_{SVC} \Delta V_{SVC} \quad (3.66)$$

The network equation of the svc bus will be modified as

$$\begin{aligned} 0 = & \frac{\partial Q_{Li}(V_i)}{\partial V_i} \Delta V_i - \left[\sum_{k=1}^n V_{ko} Y_{ik} \sin(\theta_{io} - \theta_{ko} - \alpha_{ik}) \right] \Delta V_i - \left[\sum_{\substack{k=1 \\ \neq i}}^n V_{io} V_{ko} Y_{ik} \sin(\theta_{io} - \theta_{ko} - \alpha_{ik}) \right] \Delta \theta_i \\ & - V_{io} \sum_{k=1}^n [Y_{ik} \sin(\theta_{io} - \theta_{ko} - \alpha_{ik})] \Delta V_k - V_{io} \sum_{\substack{k=1 \\ \neq i}}^n [V_{ko} Y_{ik} \cos(\theta_{io} - \theta_{ko} - \alpha_{ik})] \Delta \theta_k \\ & + \left[-2V_{SVC} x_3 \Delta V_{SVC} - V_{SVC}^2 \Delta x_3 \right] \end{aligned} \quad (3.67)$$

Correspondingly the C'_{2SVC} and D'_{22SVC} will be modified. Modifications needed for incorporating SVC's state space model into the system state space are as shown below

$$\begin{bmatrix} \Delta \dot{x} \\ \Delta \dot{x}_{SVC} \\ 0 \\ 0 \end{bmatrix} = \begin{bmatrix} A' & 0 & B_1 & B_2 \\ 0 & A_{SVC} & 0 & B_{SVC} \\ C_1' & 0 & D_{11}' & D_{12}' \\ C_{2SVC}' & 0 & D_{21}' & D_{22SVC}' \end{bmatrix} \begin{bmatrix} \Delta x \\ \Delta y_c \\ \Delta y_b \end{bmatrix} \quad (3.68)$$

By eliminating the algebraic equations A_{SVC} Matrix is obtained,

$$[A_{SYS}] = \begin{bmatrix} A' & 0 \\ 0 & A_{SVC} \end{bmatrix} - \begin{bmatrix} B_1 & B_2 \\ 0 & B_{SVC} \end{bmatrix} [J_{AE}']^{-1} \begin{bmatrix} C_1' & 0 \\ C_{2SVC}' & 0 \end{bmatrix} \quad (3.69)$$

Eigen values of the A_{SYS} matrix are computed to predict the stability of the system.

3.5 COMPUTATION OF INITIAL CONDITIONS

To compute the matrix A_{sys} it is necessary to compute the initial values for all the dynamic states. In power system dynamic analysis, the initial conditions are normally found from a base case load flow solution.

Step 1: The first step in calculation of initial conditions is the calculation of the generator

$$\text{currents as, } I_{Gi} = \frac{P_{Gi} - jQ_{Gi}}{V_i^*} \quad (3.70)$$

$$\text{Step 2: } \delta_i \text{ is computed as } \delta_i = \text{Angle of } \left(V_{ie}^{j\theta_i} + (R_{si} + jX_{qi}) I_{Gi} e^{j\gamma_i} \right) \quad (3.71)$$

Step 3: Compute $I_{di}, I_{qi}, V_{di}, V_{qi}$ as,

$$I_{di} + jI_{qi} = I_{Gi} e^{j(\gamma_i - \delta_i + \pi/2)} \quad (3.72)$$

$$V_{di} + jV_{qi} = V_i e^{j(\theta_i - \delta_i + \pi/2)} \quad \text{for } i=1, \dots, m \quad (3.73)$$

$$\text{step 4: compute } E'_{di} \text{ as, } E'_{di} = V_{di} + R_{si} I_{di} - X'_{qi} I_{qi} \quad i = 1, \dots, m \quad (3.74)$$

$$\text{Step 5: Compute } E'_{qi} \text{ as, } E'_{qi} = V_{qi} + R_{si} I_{qi} - X'_{di} I_{di} \quad i = 1, \dots, m \quad (3.75)$$

$$\text{Step 6: Compute } E_{fdi} \text{ as } E_{fdi} = E'_{qi} + (X_{di} - X'_{di}) I_{di} \quad i = 1, \dots, m \quad (3.76)$$

The above equations are used for calculating the eigen values of the systems

LOCATION OF SVC AND SELECTION OF INPUT SIGNALS

The study system used in this work comprises of 3 machines, 10 buses and 10 lines. No machine has power system stabilizer (PSS), and each machine model has its own exciter. Each machine has same type of exciter model (i.e. static exciter model). The power system network diagram is shown in figure 4.1. The system data [4] used for the study is given in APPENDIX A.

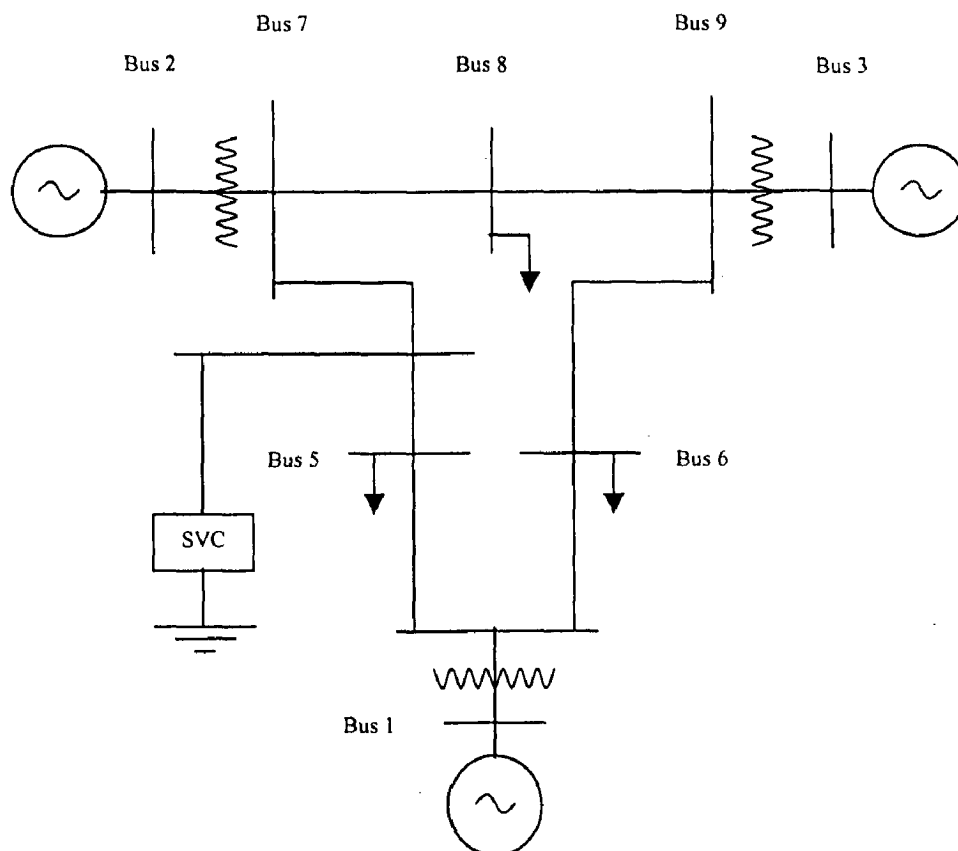


Figure 4.1: 3 Machine 10 Bus power system network diagram

4.1 PLANNING AND PREPARING THE SYSTEM MODEL FOR THE DESIGN OF CONTROLLER

It is found in open literature as well as in practice that the damping of the system decreases as the system is heavily loaded. The effective damping contribution of the SVC damping controller depends on its location and the selection input signals.

In order to show the effectiveness of the damping controller the study is conducted on two different operating conditions which are extremely apart; one base case (normal) operating condition and the other at heavily loaded (stressed) operating condition near the point of collapse which may assumed to be occurring on the system. In order to obtain more meaningful realistic study, the system includes the following characteristics:

1. Heavy power transfer,
2. Multiple areas,
3. Realistic area Dynamics, and
4. Two operating conditions.

A very systematic problem formulation is followed in order to obtain the system dynamic model.

1. Load flow is conducted for both operating conditions
2. Location of SVC and input signals to the damping controller are selected
3. Reduced order model of the system is obtained
4. Objectives and constraints of the controller are enumerated
5. Damping controller is designed and tuned for robustness
6. Controller performance is verified for both of the operating conditions.

The Load flow solutions of the system are obtained for two operating conditions with and without SVC in both the cases are presented in the chapter 2 and results are shown in APPENDIX B. SVC Location is chosen based on bus participation factors and input signals to the controller are selected based on observability controllability residues of the various possible local input signals. Reduced order model of the system is obtained for ease of analysis and design. Finally the design process is carried out using residue method and controller is tuned for robustness.

4.2 LOCATION OF SVC FOR EFFECTIVE DAMPING USING MODAL ANALYSIS [24, 25]

The location of SVC is based on the determination of critical eigen values corresponding to voltage instability under the stressed operating condition. Critical modes are computed by studying the system modes in the vicinity of the point of collapse. Eigen vectors of the critical eigen value give the information about the combination of loads responsible for the voltage collapse. System bus participation factors are used to determine the most suitable location for the SVC.

The most critical modes of the system can be computed by performing a point of collapse power flow solution, which requires the computation of system jacobian matrix at the point of maximum loadability. Modal or eigen value analysis of the system jacobian matrix near the point of collapse can be used to identify buses vulnerable to voltage collapse and locations where injections of power benefit the system most. The eigen vectors of the critical eigen value give the information about the loads responsible for the voltage collapse. The linearized relationship between the load voltage and reactive power load is expressed as

$$\lambda \Delta V = \Delta Q \quad (4.1)$$

Where λ is the V-Q sensitivity in general this sensitivity can be obtained from system jacobian matrix. When λ is close to zero, a small change in load results in large change in the voltage. Modal voltage is a particular combination of reactive power loads given by the corresponding left and right eigen vectors. The participation of each load in forming the critical mode determines the importance of the load in collapse. The degree of participation of loads is determined from an inspection of the entries of the left eigenvector of the critical mode. Larger eigen vector entries signify locations most suitable for voltage support.

$$\Delta Q = J_R \Delta V \quad (4.2)$$

$$J_R = \xi \Lambda \eta \quad (4.3)$$

where J_R is the reduced jacobian matrix,

ξ and η are the left and right eigen matrices respectively and

Λ represents the system eigen values of the jacobian matrix.

The Bus participation factor of bus 'k' in the critical mode 'i' is

$$P_{ik} = \xi_{ki} \eta_{ik} \quad (4.4)$$

Identifying critical mode is not trivial. the magnitude of eigen value is only a relative measure of proximity to instability as the system approaches collapse, the eigen values that initially have small real component may not be critical, and other eigen values may become critical. For the stressed case operating condition of power system eigen vales of jacobian matrix obtained are the critical modes of voltage instability given in the following table 4.1

Eigen values of jacobian matrix

Mode no	eigenvalue
1	58.2529
2	48.2495
3	44.3082
4	28.1373
5	20.1470
6	0.0938
7	13.6454
8	4.7803
9	7.4388

Table 4.1: eigen values of jacobian matrix at the point of system voltage collapse

Bus Participation Factors

	λ_1	λ_2	λ_3	λ_4	λ_5	λ_6	λ_8	λ_9	λ_{10}
2	0.0958	0.0048	0.0192	0.0335	0.2753	0.1402	0.1092	0.0802	0.2419
3	0.0081	0.1199	0.1092	0.0030	0.1516	0.1117	0.1137	0.3825	0.0002
4	0.0016	0.2785	0.4406	0.0891	0.0021	0.0298	0.0307	0.0030	0.1247
5	0.0091	0.0732	0.0935	0.2365	0.0101	0.1104	0.0993	0.1098	0.2582
6	0.0004	0.0772	0.0195	0.0683	0.0010	0.0599	0.5358	0.0372	0.2007
7	0.6220	0.0177	0.0548	0.0162	0.0114	0.1487	0.0042	0.0441	0.0808
8	0.1332	0.0277	0.0071	0.0712	0.5421	0.1432	0.0002	0.0083	0.0669
9	0.0441	0.3697	0.2554	0.0011	0.0032	0.1129	0.0059	0.2076	0.0001
10	0.0857	0.0312	0.0007	0.4812	0.0032	0.1431	0.1010	0.1273	0.0266

Table 4.2: Bus participation factors of the system for all modes of voltage instability

From the bus participation factors shown in table 4.2, it is observed that the area corresponding to buses 2, 7, 8, 10 near the second machine are the buses most vulnerable to instability. But it is proved [1] that the best location for installation of SVC is the mid-point of transmission line (instead of a generator bus 2 or 7), where the voltage variations are maximum without SVC. Therefore mid-point located SVC can best support the system from voltage instability by suitable reactive power compensation. From the table 4.2 the bus participation factors corresponding to buses 8 and 10 have almost same values. Therefore, either bus 8 or 10 can be selected as the best location for installing SVC. In this work, a SVC has been installed at bus number 10.

4.3 SELECTION OF INPUT SIGNALS FOR THE CONTROLLER [2, 35]

Locally measurable quantities can be used for identifying the inter area modes of oscillations which shows good observability of the modes of the system can be used as input signals to the controller. The possible local measurements that can be selected as input signals to the controller are as follows

$$Y = CX \quad (4.5)$$

$$Y = \begin{bmatrix} \Delta I_{ik} \\ \Delta P_{ik} \\ \Delta Q_{ik} \end{bmatrix} \quad (4.6)$$

Line current magnitude (ΔI_m) can be expressed in terms of states of the system (ΔX) as

$$\begin{aligned} I_{ik} &= Y_{ik}(V_i - V_k) \\ I_{ik} &= (G_{ik} + jB_{ik})\{(V_i \cos(\delta_i) - V_k \cos(\delta_k)) + j(V_i \sin(\delta_i) - V_k \sin(\delta_k))\} \\ I_{ik}^2 &= (G_{ik}^2 + B_{ik}^2)\{V_i^2 + V_k^2 - 2V_i V_k \cos(\delta_i - \delta_k)\} \end{aligned} \quad (4.7)$$

Linearizing the above equation

$$\begin{aligned} 2I_{ik} |\Delta I_{ik}| &= (G_{ik}^2 + B_{ik}^2)\{2V_i \Delta V_i + 2V_k \Delta V_k - 2\{(V_k \cos(\delta_i - \delta_k) \Delta V_i \\ &+ V_i \cos(\delta_i - \delta_k) \Delta V_k - V_i V_k \sin(\delta_i - \delta_k) \Delta \delta_i + V_i V_k \sin(\delta_i - \delta_k) \Delta \delta_k)\}\} \end{aligned} \quad (4.8)$$

From the equation (3.47), ΔV can be expressed in terms of ΔX ,

$$\Delta V = [M] \Delta X \quad (4.9)$$

$$\text{where } [M] = -[JAE]^{-1} [C]$$

$$|\Delta I_{ik}| = (G_{ik}^2 + B_{ik}^2) \{ (V_i - V_k \cos(\delta_i - \delta_k)) \Delta V_i + (V_k - V_i \cos(\delta_i - \delta_k)) \Delta V_k + V_i V_k \sin(\delta_i - \delta_k) \Delta \delta_i - V_i V_k \sin(\delta_i - \delta_k) \Delta \delta_k \} / \Delta I_{ik} \quad (4.10)$$

The above equation can be expressed in terms of ΔX

$$|\Delta I_{ik}| = (G_{ik}^2 + B_{ik}^2) \{ (V_i - V_k \cos(\delta_i - \delta_k)) M_{Vi} + (V_k - V_i \cos(\delta_i - \delta_k)) M_{Vk} - V_i V_k \sin(\delta_i - \delta_k) M_{\delta} + V_i V_k \sin(\delta_i - \delta_k) M_{\delta_k} \} / \Delta I_{ik} \Delta X \quad (4.11)$$

$$\Delta I_m = [C_1] \Delta X \quad (4.12)$$

$$\Delta P_{ik} = (Y_{ik} V_k \cos(\delta_i - \delta_k - \alpha_{ik})) \Delta V_i + (Y_{ik} V_i \cos(\delta_i - \delta_k - \alpha_{ik})) \Delta V_k - (V_i Y_{ik} V_k \sin(\delta_i - \delta_k - \alpha_{ik})) \Delta \delta_i + (V_i Y_{ik} V_k \sin(\delta_i - \delta_k - \alpha_{ik})) \Delta \delta_k \quad (4.13)$$

$$\Delta P_{ik} = \{ (Y_{ik} V_k \cos(\delta_i - \delta_k - \alpha_{ik})) M_{Vi} + (Y_{ik} V_i \cos(\delta_i - \delta_k - \alpha_{ik})) M_{Vk} - (V_i Y_{ik} V_k \sin(\delta_i - \delta_k - \alpha_{ik})) M_{\delta} + (V_i Y_{ik} V_k \sin(\delta_i - \delta_k - \alpha_{ik})) M_{\delta_k} \} \Delta X \quad (4.14)$$

$$\Delta Q_{ik} = (Y_{ik} V_k \sin(\delta_i - \delta_k - \alpha_{ik}) + 2V_i Y_{ik} \sin(\alpha_{ik})) \Delta V_i + (Y_{ik} V_i \sin(\delta_i - \delta_k - \alpha_{ik})) \Delta V_k + (V_i Y_{ik} V_k \cos(\delta_i - \delta_k - \alpha_{ik})) \Delta \delta_i - (V_i Y_{ik} V_k \cos(\delta_i - \delta_k - \alpha_{ik})) \Delta \delta_k \quad (4.15)$$

$$\Delta Q_{ik} = \{ (Y_{ik} V_k \sin(\delta_i - \delta_k - \alpha_{ik}) + 2V_i Y_{ik} \sin(\alpha_{ik})) M_{Vi} + (Y_{ik} V_i \sin(\delta_i - \delta_k - \alpha_{ik})) M_{Vk} - (V_i Y_{ik} V_k \cos(\delta_i - \delta_k - \alpha_{ik})) M_{\delta} + (V_i Y_{ik} V_k \cos(\delta_i - \delta_k - \alpha_{ik})) M_{\delta_k} \} \Delta X \quad (4.16)$$

Arranging these three signals in matrix form

$$Y = [C] \Delta X$$

$$\begin{bmatrix} \Delta I_{ik} \\ \Delta P_{ik} \\ \Delta Q_{ik} \end{bmatrix} = \begin{bmatrix} C_1 \\ C_2 \\ C_3 \end{bmatrix} [\Delta X] \quad (4.17)$$

The state space representation of power system is

$$\begin{aligned} \dot{X} &= AX + BU \\ Y &= CX \end{aligned} \quad (4.18)$$

The equivalent system representation in modal form is given by

$$\begin{aligned} \dot{Z} &= [\Lambda]Z + [T^{-1}B]U \\ Y &= [CT]Z \\ \dot{Z}_i &= \lambda_i Z + \sum_{k=1}^n [T^{-1}]_i [B]_k U_k \end{aligned} \quad (4.19)$$

where λ_i is the i^{th} eigen value of the system and $[T^{-1}]_i$ is the i^{th} row of left eigen matrix $[B]_k$ is the k^{th} column of the B matrix. The open loop Transfer Function of the power system can be obtained as

$$G(s) = \frac{Y}{U} = C[sI - As]^{-1} B \quad (4.20)$$

$$= [CT][sI - \Lambda]^{-1} [T^{-1}B] \quad (4.21)$$

$$Z_i = \lambda_i Z + \sum_{k=1}^n \beta_{ik} U_k \quad (4.22)$$

Where β_{ik} indicates the controllability of the i^{th} mode, in other words β_{ik} means the effect of k^{th} input on i^{th} mode[24].

$$Y = [CT]X \quad (4.23)$$

The measure of mode observability of a certain mode i from the local line signal is given by $[CT]$. The open loop transfer function of the power system can be expressed in terms of modes and residues

$$G(s) = \sum_{i=1}^n \frac{R_{ij}}{(s + \lambda_i)} \quad (4.24)$$

$$R_{ij} = \lim_{s \rightarrow \lambda_i} (s + \lambda_i) G(s) \quad (4.25)$$

R_{ij} is the residue associated with i^{th} mode and j^{th} transfer function and can be expressed in mode controllability and observability

$$R_{ij} = [CT][T^{-1}B] \quad (4.26)$$

$$R_{ij} = \text{Ctrb}_{ij} * \text{Obsv}_{ij} \quad (4.27)$$

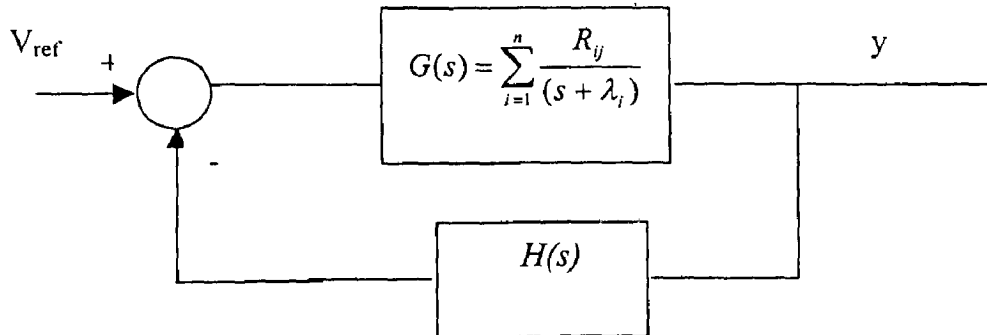


Fig: 3.1: Block diagram representation of closed loop system

Adding the feedback loop will cause a change in the i^{th} eigen value[35]. The closed loop poles are give by

$$1 + G(s) H(s) \quad (4.28)$$

$$(s+\lambda_i) + R_{ij} * H(s) \quad (4.29)$$

$$(s+\lambda_i) + \Delta\lambda \quad \text{Where } \Delta\lambda = R_{ij} * H(s)$$

Therefore a damping controller with j^{th} input signal having largest residue for i^{th} mode will cause largest change in λ_i . The local signal which has large residue value can be selected as the best input signal to the controller.

The residue values of the three input signals obtained from the system under consideration are

	Line 10-7	Line 10-5
ΔI_m	4.7973	4.1572
ΔP	4.2467	3.4108
ΔQ	3.9461	1.5634

Table 4.3: Residue values of the line measurements

Therefore line current magnitude signal ΔI_m in the line 10-7 is taken as input signal to the controller which shows largest residue value.

DESIGN OF DAMPING CONTROLLER FOR SVC

5.1 MODEL ORDER REDUCTION [26, 32]

Detailed mathematical modeling of the system is very difficult to analyze as it contains too many oscillatory modes of the system. Reduced model order of the system can be obtained for ease of analysis and design of control system.

5.1.1 OBJECTIVES OF MODEL ORDER REDUCTION

In the present 3-Machine, 10-Bus system the full detailed mathematical model consists of 18 states, 5 states for each machine and 3 states for SVC, which is large in dimension and needs to be reduced for the following reasons.

1. Large scale system is very difficult for both analysis and design of control system.
2. Large dimensional system in state space form requires large computer storage and more simulation time.
3. Controller based on large dimensional state vector is neither economical nor reliable.
4. A very detailed mathematical model of the system consists of higher order differential equations which are difficult to solve in general.

5.1.2 MODEL ORDER REDUCTION OF THE SYSTEM

A reduced order model of the system, which retains the important characteristics of the original higher order system, can replace the original system. A reduced order model should approximately have the same time and frequency as that of the original system. The reduced order model of a system in state space form can be obtained by eliminating some of the states from the higher order system. A systematic procedure is followed in order to obtain the reduced order model of the system which mimics the original system.

1. Elimination of zero eigen value [19]

In the multi machine model developed in the previous chapter, absolute rotor angles are taken as state variables; there will be a zero eigen value present in the model. This arises because the sum of the columns in the A matrix corresponding to δ 's will add up to zero. It

can be suppressed by taking the angle differences instead of absolute angles as the state variables. This reduces the order of the system by one. If the r^{th} machine is taken as the reference, the required changes in A can be achieved by deleting the row and column corresponding to $\Delta\delta_r$ and placing -1 in the intersections of the rows corresponding to other $\Delta\delta$'s and column corresponding to $\Delta\omega_r$.

2. Pole Zero cancellation [5]

If the system is not completely state controllable and observable, that means that there exists a sub-system which is disconnected or in other words isolated from the input and output variables. The cancelled modes can't be controllable and observable. A minimal realized system achieved by pole zero cancellation is completely controllable and observable. There is one pole zero combination which can be cancelled in the open loop system transfer function of the power system. This reduces the order of the system by one.

3. Elimination of infinitely fast states

As the measuring and control time constants (T_m, T_c) of the SVC are very small the corresponding state variables x_1 and x_3 of the SVC can be treated as infinitely fast acting states, in other words these states can be approximated to instantaneously measurable and controllable states, which can be eliminated from the system obtained from step 2. In this step the order of the system is reduced by two.

4. Elimination of weakly coupled states

Hankel singular values can be computed from balanced realization of the system represented in state space form. Very small Hankel singular values indicates that the associated states are weakly coupled between the input and output variables which can be eliminated. This is done as follows, the state vector can be partitioned into two parts X_1 which can be retained, X_2 which can be eliminated

$$\begin{bmatrix} \dot{X} \\ 0 \end{bmatrix} = \begin{bmatrix} A_{11} & A_{12} \\ A_{21} & A_{22} \end{bmatrix} \begin{bmatrix} X_1 \\ X_2 \end{bmatrix}$$

The derivative of fast states X_2 can be made equal to zero, and then solved for the remaining state equations X_1 . In the three machine ten bus system considered in this work there are five states whose Hankel singular values are very small they have been eliminated by the above method. This reduces the order of the system by five. The final reduced order model of the system contains 9 states,

5.1.3 THE STEP RESPONSE OF THE HIGHER ORDER AND REDUCED ORDER MODEL OF THE SYSTEM

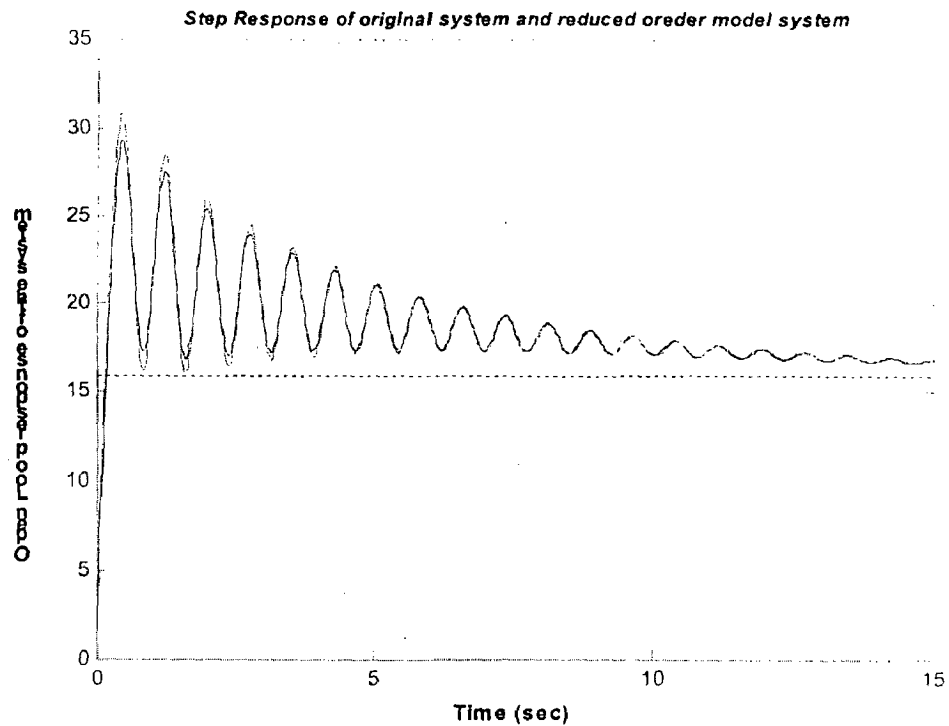


Figure 5.1: comparing the open loop step response of original higher order system and reduced order system

The step response of the original system and reduced order system for base case operating condition are shown in figure 5.1. The original system contains 17 states after eliminating zero eigen value and the reduced order model of the system contains 9 states, which is completely controllable and observable and stable. This model is very easy to analyze and to design the control system. In the root locus plane it is easy to tune for optimal damping compared to original higher order system. From the response plot it is observed that the reduced order model of the system contains all the important characteristics of the original higher order system. Fig. 5.1 shows the validity of the reduced order model of the system that can be used to replace the original higher order system. The step responses of the open loop transfer function of the system between line current magnitude ΔI_m and ΔV_{SVCref} are shown for comparison of the original and reduced order model systems.

5.2 DESIGN OF DAMPING CONTROLLER [4, 7, 31, 33, 35, 37]

5.2.1 OBJECTIVE AND CONSTRAINTS OF DAMPING CONTROLLER

The objective of the damping controller is to improve the over all dynamic stability of the system by providing damping for poorly damped modes of oscillations.

The constraints on the design are:

1. The damping controller must coordinate with the other system controls (generation dispatch; load frequency control; voltage control).
2. Control action shall not cause excessive variation in major system variables; e.g., voltage, power, speed, frequency.
3. The controller designed based on linearized model should not interfere the transient controls of the system
4. The controller should give satisfactory performance for diverse operating conditions.

5.2.2 COMPONENTS OF DAMPING CONTROLLER

The basic function of damping controller is to add damping to the poorly damped modes of oscillations by controlling its terminal voltage using auxiliary control signals. In order to provide damping the controller must produce a component of torque in phase with the dynamic oscillations of input signals. In practice, line current flow (ΔI_{line}) and SVC voltage regulator input (ΔV_{SVCref}) exhibit frequency dependent gain and phase characteristics. Therefore the damping controller to be designed should contain appropriate phase compensation circuits to compensate for the phase lag between voltage regulator input (ΔV_{SVCref}) and the line current (ΔI_{line}) flow. In ideal case, with the phase characteristics of the damping controller should be an exact inverse of the voltage regulator input (ΔV_{SVCref}) and line current (ΔI_{line}) flow phase characteristic. The damping controller would result in a pure damping torque at all oscillating frequencies of the range of interest. The damping controller is required to contribute to damping of the rotor oscillations over a range of frequencies rather than for a single frequency. Block diagram of the damping controller is shown in fig.5.2.

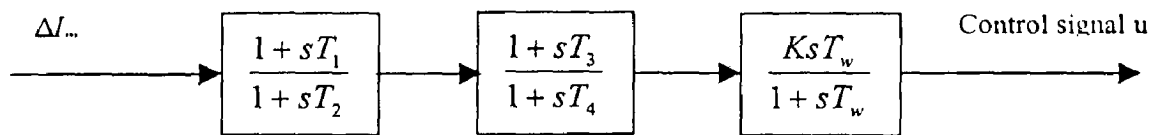


Figure 5.2: Block diagram of damping controller

1. **Phase compensation (T_1, T_2, T_3, T_4)**

This block provides the appropriate phase lead characteristic to compensate for phase lag between the voltage regulator input (ΔV_{SVCref}) and the line current flow (ΔI_{line}). Normally the phase lead network should provide compensation over the frequency range of 0.1-2.0 Hz. The amount of phase compensation changes with the system conditions.

2. **The signal washout block (T_w)**

It serves as a high pass filter with the time constant T_w enough to allow signals associated with oscillations in ΔI_m to pass unchanged, without it, steady changes in line current would modify the error signal. It allows the damping controller to respond to the changes in current only.

3. **Damping controller gain (K)**

The gain has an important effect on damping of the oscillations. The value of gain is chosen by examining its effect over a wide range of values. The damping increases with increase in gain up to certain value beyond which further increase in gain will reduce the damping. Ideally gain K should be set at a value corresponding to max damping. Most of the cases K is chosen as 1/3 of the critical eigen value.

5.2.3 METHOD OF DESIGN OF DAMPING CONTROLLER [35]

The open loop transfer function of the power system can be expressed in terms of modes and residues

$$G(s) = \sum_{i=1}^n \frac{R_{ij}}{(s + \lambda_i)} \quad (5.2)$$

$$R_{ij} = \lim_{s \rightarrow \lambda_i} (s + \lambda_i) G_j(s) \quad (5.3)$$

R_{ij} is the residue associated with i^{th} mode and j^{th} transfer function and can be expressed in mode controllability and observability

$$R_{ij} = [CT][T^{-1}B] \quad (5.4)$$

$$R_{ij} = \text{Ctrb}_{ij} * \text{Obsv}_{ij} \quad (5.5)$$

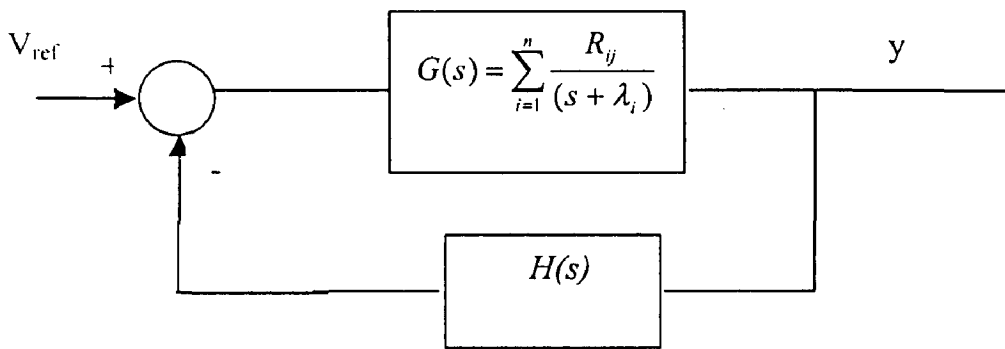


Fig: 5.3 Block diagram representation of closed loop system

Adding the feedback loop will cause a change the i^{th} eigen value[35]. The closed loop poles are give by

$$1 + G(s) H(s) \quad (5.6)$$

$$(s + \lambda_i) + R_{ij} * H(s) \quad (5.7)$$

$$(s + \lambda_i) + \Delta\lambda \quad \text{Where } \Delta\lambda = R_{ij} * H(s) \quad (5.8)$$

In the case of pure gain feedback without any compensation the eigen value of the closed loop system will modify the real part and imaginary part of the eigen value is given by the expression (5.8).

$$\begin{aligned} \text{i.e, when } H(s) = K \text{ then } \Delta\lambda &= K * R_{ij} \\ &= K * R_{ij} (real + J Imag) \end{aligned}$$

When the phase characteristic is exactly compensated then pure damping can be added to the mode without modifying the phase angle of the mode. Therefore from the residue value the required amount of phase compensation can be obtained. A single stage phase lead compensator is designed which is valid well up to 60° of phase compensation. If the amount of compensation required is more than 60° then multiple stages of same compensator blocks are cascaded for obtaining the required amount of phase compensation. The single stage phase lead compensator design steps are as follows
The pole-zero spread of the compensator is obtained from the required amount of phase angle compensation Φ_{ij}

$$a = \frac{(1 - \sin \phi_{ij})}{(1 + \sin \phi_{ij})} \quad (5.9)$$

The time constants of the compensator block are

$$\begin{aligned} T_1 &= \frac{1}{\omega_m \sqrt{a}} \\ T_2 &= aT_1 \end{aligned} \quad (5.10)$$

where ω_m is the centre frequency where the peak value of the compensation occurs

The total overall transfer function of the feedback path appears as

$$H(s) = K \frac{sT_w}{(1 + sT_w)} \left[\frac{(1 + sT_1)}{(1 + sT_2)} \right]^m \text{ (FILTER)} \quad (5.11)$$

where 'm' is the no. of stages of the compensator

The filter can be used to filter the noise signals and for rejecting the range of modes of the system corresponding to sub-synchronous torsional band to avoid adverse interaction with these mode.

5.2.4 TUNING OF THE DAMPING CONTROLLER [28, 34, 37]

The initial direction of eigen value migration as gain is increased from zero is determined by the phase at the local mode frequency. For perfect compensation, $\phi_L=0$ Pure damping will be added and the eigen value will move directly into the left half plane with no change in frequency. If phase lag exists, the frequency will increase in proportion to the amount of damping increase, given by the following expression

$$\tan \phi_L = -\frac{\Delta \omega_L}{\Delta \sigma_L} \quad (5.13)$$

where ω_L is the local mode frequency

σ_L is the local mode decay rate

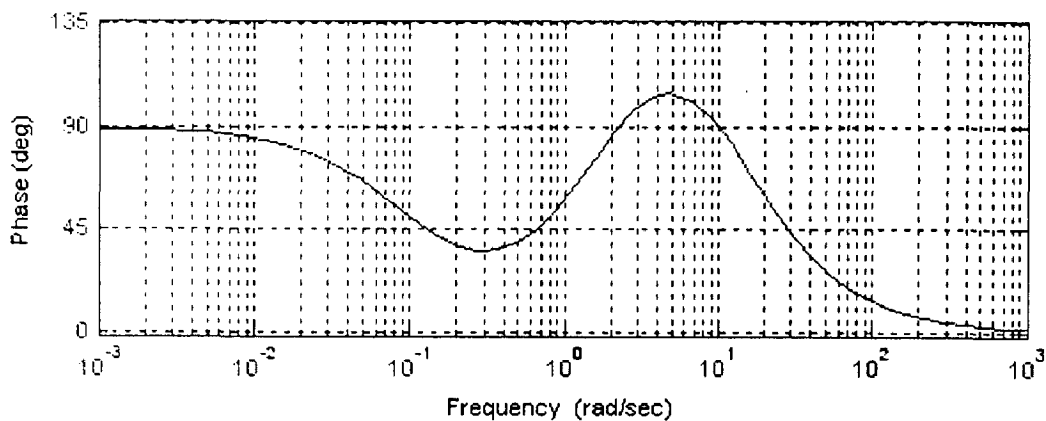


Figure 5.4: Bode plot of the compensator

For $\Phi_L= 45$ the frequency will increase at the same rate as the damping, and for $\Phi_L= -90$, no change in damping will take place, but frequency will increase. This analysis is very important in the tuning stage of the controller in the root locus plane for optimum damping.

RESULTS AND CONCLUSIONS

6.1 RESULTS

The damping of the system decreases as the system is heavily loaded. So, It is very important to ensure the damping of the system under heavily loaded operating condition near the point of collapse. The damping controller has been designed for inter area modes of oscillation of the system for stressed case operating condition.

The damping controller is designed using observability controllability residue method. The damping controller is designed and tuned based on reduced order model of the system and the results are shown on the original higher order system applying damping controller.

The eigen values of the higher order system applying damping controller are presented in table 6.1 for stressed case operating condition. Table 6.2 shows the eigen values of the original higher order system without SVC, with SVC, and with SVC damping controller.

Without SVC	With SVC	With SVC damping controller
-0.8569 +12.6975i	-0.6406+12.7798i	-0.6849+12.7856i
-0.8569-12.6975i	-0.6406-12.7798i	-0.6849-12.7856i
-0.2988+8.0069i	-0.1123+8.2348i	-0.2486+8.1593i
-0.2988-8.0069i	-0.1123-8.2348i	-0.2486-8.1593i
-0.0758+6.4258i	-3.0649+3.2461i	-4.7803+5.0831i
-0.0758-6.4258i	-3.0649-3.2461i	-4.7803-5.0831i
-0.1359	-4.5255+1.2496i	-4.4435+1.1707i
-4.4994+1.2475i	-4.5255-1.2496i	-4.4435-1.1707i
-4.4994-1.2475i	-4.4556	-4.4417
-4.3736	-0.1428	-2.4321+1.4697i
-1.2974	-2.6055+1.5845i	-2.4321-1.4697i
-2.7647+1.2832i	-2.6055-1.5845i	-1.2154
-2.7647-1.2832i	-1.2164	-0.1280
-3.2258	-3.2258	-0.0996
	-81.7535	-3.2258
	-5.1339+30.1877i	-79.3136
		-8.3965+32.7296i
		-8.3965-32.7296i
		-6.6633

Table 6.1 : Eigen values of system for stressed case operating condition

Without SVC	With SVC	With SVC Damping controller
-0.8481 +12.7647i	-0.8171 +12.7469i	-0.8281+12.7726i
-0.8481 -12.7647i	-0.8171 -12.7469i	-0.8281-12.7726i
-0.2509 + 8.3637i	-0.2902 + 8.1721i	-0.4772+8.8628i
-0.2509 - 8.3637i	-0.2902 - 8.1721i	-0.4772-8.8628i
-2.2411 + 3.0194i	-2.1478 + 2.9317i	-2.1966+2.9107i
-2.2411 - 3.0194i	-2.1478 - 2.9317i	-2.1966-2.9107i
-4.6669 + 1.3818i	-4.6836 + 1.3734i	-4.7008+1.3811i
-4.6669 - 1.3818i	-4.6836 - 1.3734i	-4.7008-1.3811i
-0.1363	-0.1441	-3.5883
-3.4863 + 0.9991i	-3.1964 + 0.6390i	-2.8571+0.5293i
-3.4863 - 0.9991i	-3.1964 - 0.6390i	-2.8571-0.5293i
-2.2618	-2.8495	-0.1279
-0.8873	-0.8954	-0.0998
-3.2258	-3.2258	-0.8945
	-14.9967 +13.6840i	-3.2258
	-70.1185	-19.6108 +21.0013i
	-14.9967 +13.6840i	-67.4854
		-19.6108 -21.0013i
		-6.8338

Table 6.2 : eigen values of the system for base case operating condition

The transfer function of the system is obtained between input V_{ref} and output I_{line} from the mathematical modeling of multi machine power system. The step response of the transfer function is shown in figure 6.1.

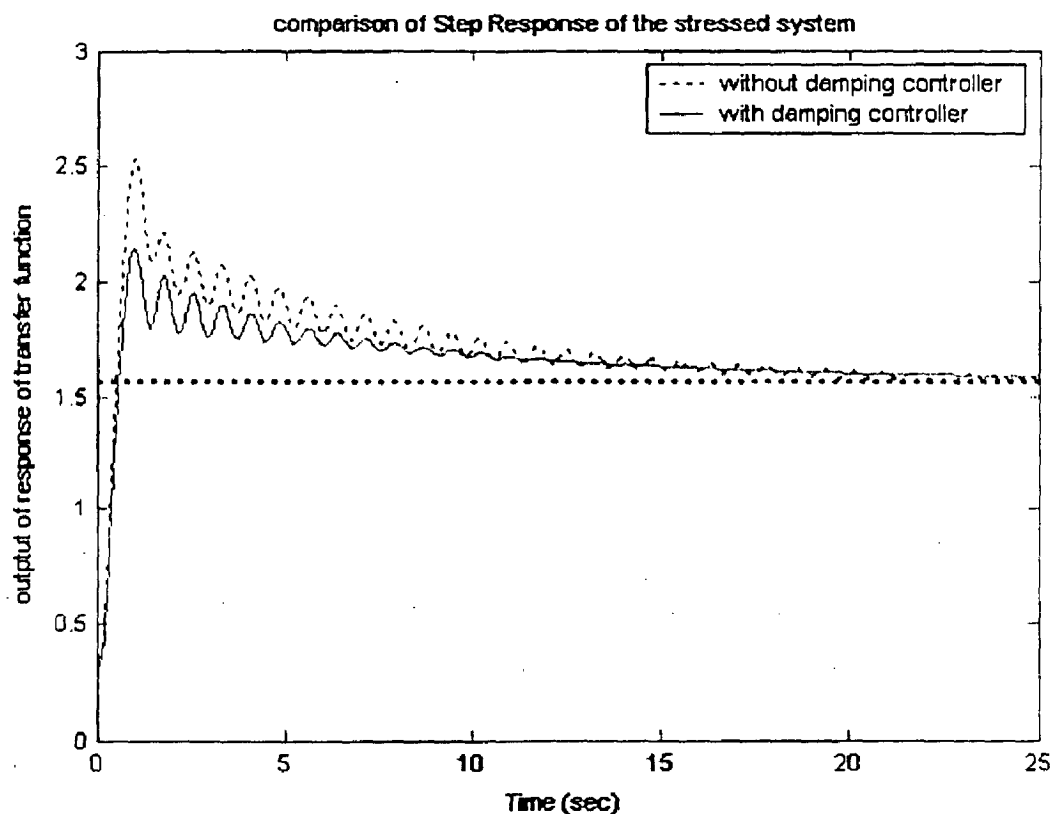


Figure 6.1: comparison of step response of the original higher order system for stressed case operation

Figure 6.1 Compares the step response of Open Loop Transfer Function of the system without damping controller (indicated by dashed lines) and step response of Closed Loop Transfer Function with damping controller for stressed case operating condition, which shows that the damping of the system is improved with the damping controller.

The step response of the system with and without damping controller for heavily loaded condition is shown in the figure 6.1. The same damping controller is applied for base case operation of the system, the step response is shown in figure 6.2, both response plots shows the improvement in damping of the system. The controller designed based on stressed case operation is satisfactory for base case operating condition also without adding any adverse side effects.

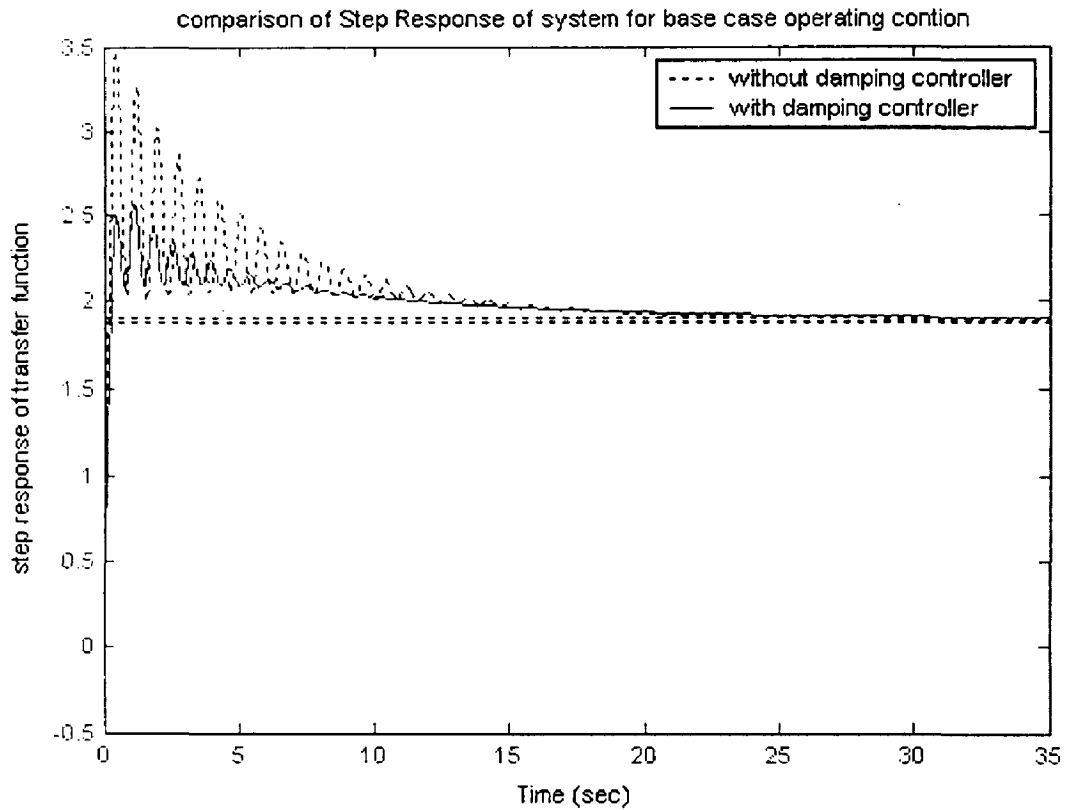


Figure 6.2: comparison of step response of the original higher order system for base case operation

Figure 6.2 compares the step response of Open Loop Transfer Function of the system without damping controller (indicated by dashed lines) and step response of Closed Loop Transfer Function with damping controller for base case operating condition, which shows that the damping of the system is improved with the damping controller.

From the figures 6.1 and 6.2, it can observed that the oscillations in line current between buses 10 and 7 is effectively damped out.

6.2 DISCUSSION

1. Robustness of the designed controllers [35]

A robust controller is expected to perform satisfactorily at various operating conditions. However, since the proposed controller has been designed using linear analysis of the power system, it is important to check that it performs satisfactorily when disturbances occur. The robustness of the controller is evaluated in two different ways. The first is to evaluate the system performance and damping ratio of critical modes of the system under a heavily stressed operating condition compared to the original operating condition. The second way is to evaluate the system response to various disturbances using time domain simulation of the nonlinear power system model.

2. Coordination with Other Controls [32]

Certain inherent design characteristics of the Damping Controller provide good coordination with the generation dispatch; load frequency; and voltage control systems; as follows:

- 1 . The damping controller provides no control signals to the turbines (steam, gas, hydro) in the system. In addition, the damping controller provides no steady-state control signals to the generators.

- 2 . The control signals to the SVC voltage regulator are inherently supplementary, by using rate type wash-outs on the line current measurements used by the gain of the damping controller.

The first inherent design characteristic means that the damping controller has no steady-state effect on generation control. The second inherent characteristic means that the damping controller has no steady-state effect on system voltage control.

6.3 CONCLUSIONS

The damping controller is designed using observability controllability residue method. The damping controller is designed and tuned based on reduced order model of the system and the results are shown on the original higher order system applying damping controller.

The damping controller is designed for inter area modes of oscillation for two operating conditions which are extremely apart covering the entire range of operation of power system. The step response of the system for both operating conditions shows the improvement in damping of the system for both operating conditions.

Therefore, it can be concluded that the performance of the controller will be satisfactory for any other system operating point in the range between these two extreme operating cases.

REFERENCES

- [1]. R.Mohan Mathur, and R.K. Varma, Thyristor based FACTS controllers for electrical transmission systems, John Wiley & sons, inc. Publication.
- [2]. P.Kundur, power system stability and control. New York: Mc Graw hill, Inc., 1993.
- [3]. L.Gyugyi, and N.G. Hingorani, Understanding FACTS, IEEE press, New York, 1999.
- [4]. Peter W.Sauer, M.A.Pai, Power System Dynamics and stability, Pearson Education,1998.
- [5]. Katsuhiko Ogatta , Modern Control Engineering, Prentice Hall India pvt. Ltd.
- [6]. W.Li, "Acomparative study of damping schemes on damping generator oscillations", IEEE Transactions of Power Systems, Vol.-8, May 1993, pp : 613-619.
- [7]. E.V. Larsen, and J.J. Sanchez-Gasca, and J.H. Chow, "Concepts for design of FACTS controllers to damp power swings", IEEE transactions on power systems, Vol.-10, No.-2, May 1995, pp : 948-955.
- [8]. K.R.Padiyar and R.K.Varma, "Damping torque analysis of static var controllers", IEEE Transactions on Power Systems, Vol.-6, No.-2, May1991, pp : 458-465.
- [9]. J.R.Smith, and D.A.Pierre, D.A.Rudburg,A.P Johnson, "An enhanced LQ adaptive var unit controller for power system damping", IEEE Trans. on power systems, Vol.-4, No.-2, May1989, pp : 443-451.
- [10]. J.R.Smith, D.A.Pierre, I.Sadighi,M.H. Nehrir, and J.F.Hauer, "A supplementary adaptive var unit controller for power system damping", IEEE Transactions on power systems, Vol.-4, No.-2, May1989, pp : 443-451.
- [11]. Q.Zhao, and J. Jiang, "Robust SVC controller design for improving power system damping", IEEE Transactions on power system, Vol.-10, No.-4, November1995, pp : 1927-1932
- [12]. M.Parniani, and M.R. Irvani, "Optimal robust control design of SVC", IEEE transactions on power systems, Vol.-10, No.-4, November 1995, pp : 172-179.
- [13]. Hiyama T., and Hubbi W., "Fuzzy logic control scheme with variable gain for static var compensator to enhance power system stability", IEEE transactions on power systems, Vol.-114, No.-1, February 1999, pp : 186-191.

- [14]. K.A. Elithy and S.M. Al-Alwai, "Tuning a static var compensator controller over a wide range of load models using Artificial Neural Network", *Electric power systems research*, Vol.-38, No.-2, August 1996, pp : 97-104.
- [15]. P. Ju and E. Handschin and F. Reyer, "Genetic algorithm aided controller design with application to power system damping", *IEE proceedings generation, Transmission, and distribution*, Vol.-143, No.-3, May 1996, pp : 258-262.
- [16]. M.Khammash, and V.Vittal, and Xuechun Yu, "Robust design of a damping controller for static var compensator in power systems", *IEEE Transactions on power systems*, Vol.-16, N0.3, August 2001.
- [17]. H.Kwakernaak, "Robust control and H_2 optimization tutorial paper", *Automatica*, Vol.-9, No.-2, 1993, pp : 225-273.
- [18]. H.Ambriz-perez, E. Acha, and C.R.Fuerte-Esquivel, "Advanced SVC models for Newton Raphson load flow and Newton power flow studies", *IEEE Transactions on power systems*, Vol.-15, No.-1, February 2000, pp : 129-136.
- [19] Mark J Laufenberg and M A Pai and K.R.padiyar, "Hopf bifurcation control in power systems with static var compensators", *Electrical Power and Energy Systems*, Vol.-19, No.-5, October 1997, pp : 339-347.
- [20]. Angelidis G and Semlyen A, "Improved methodologies for the calculation of critical eigen values in small signal stability analysis", *IEEE Transactions on power systems*, Vol.-11, No.-3, August 1996, pp : 1209-1217.
- [21]. Yousin Tang and Meliopoulos, A.P.S, "Power system small signal stability analysis with FACTS elements", *IEEE Transactions on Power Delivery*, Vol.-12, No.-3, July 1997, pp : 1352-61.
- [22]. Yuri V. Makarov and Zhao Yang Dang and David J.Hill, "A general method for small Signal stability Analysis", *IEEE Transactions on power systems*, Vol.-13, No.-3, August 1998.
- [23]. Special Stability controls working group, "Static var compensator models for power flow and dynamic performance simulation", *IEEE Transactions on power systems*, Vol.-9, No.-1, February 1994.

- [24]. Okamoto, Hiroshi, Kurota, Atsushi, Sekine, Yashuji., "A method for Identification of effective location of variable impedance apparatus in enhancement of steady state stability in large scale power systems", IEEE transactions on power systems, Vol.-10, No.-3, August 1995, pp : 1401-1407.
- [25]. Yakout Mansour Wisun Xu, Fermanado Alvarado, "SVC placement using critical modes of Voltage instability", IEEE proc.1993.
- [26]. Kundur.p, Lei Wang, Meir Klein, Solomon Yirga, "Dynamic reduction of large power systems for stability studies", IEEE Transactions on power systems, Vol.-2, No.-12, May 1997, pp : 889-895.
- [27]. P.Kundur, M.klein, G.J.Rogers, "Application of power system stabilizer for enhancing over all system damping", IEEE Transactions on power systems, Vol.-4, No.-2, May 1989, pp : 614-626.
- [28]. P.Kundur, M.Klein, G.J.Rogers, "Analytical investigation of factors influencing performance of power system stabilizers", IEEE Transactions on Energy conversion, Vol.-7, No.-3, September 1992, pp : 382-390.
- [29]. P.Kundur, G.J.Rogers, M.Klein, "Fundamental study of inter area oscillations in power systems", IEEE Transactions on power systems, Vol.-6, No.-3, August 1994, pp : 914-921,.
- [30]. P.Kundur, G.C.Rogers, M.G.Lauby Lei Wang, D.Ywong, "A comprehensive computer program package for small signal stability analysis of power systems", IEEE Transactions on power systems, Vol.-5, No.-4, November 1990.
- [31]. Einar Larsen, Doug fisher, Niusha Rostamkolai, "Design of supplementary modulation control function for Chester SVC ", IEEE Transactions on Power delivery Vol.-8, No.-2, April1993, pp : 335-341.
- [32] S.Hirano, T.Michigami, A.Kurita, D.B.Kaplar, N.W.miller, J.J.sanchezGasca, T.D Younkings, "Functional design for a system wide multi variable damping controller", IEEE Transactions on power systems, Vol5, No.-4, November1994, pp : 1127-1136,.
- [33]. M.Noroozian, G. Anderson, "Damping of inter area and local modes by use of controllable components", IEEE Transactions on power delivery, Vol.-10, No.-4, October 1995, pp : 2007-2012.

- [34]. E.Z.Zhou, "Functional sensitivity concept and its application to power system damping control", IEEE Transactions on power systems, Vol.-9, No.-1, February 1994, pp : 518-524.
- [35]. Magdy E. Aboul-Ela, A.A.Sallam, James D. Mc Calley, A.A Fouad, "Damping controller design for power system oscillations using global signals", IEEE Transactions on power systems, Vol.-11, No.-2, May 1996, pp : 767-773.
- [36]. N. Mithulanathan, Claudio A. Canizares, John Reeve, Graham J. Rogers, "Comparison of PSS, SVC and STATCOM Controllers for Damping Power System Oscillations", IEEE Transactions on Power Systems October 2002.
- [37]. E.V. Larsen, D.A. Swarn, "Applying Power System Stabilizers: Part- I, Part -II, Part- I I", IEEE Transactions on Power Apparatus and Systems, Vol.-100, No.-6, June 1981, pp : 3017-3046.
- [38]. Glauco N. Taranto, Joe H. Chow, and Hisham A. Othman, "Robust Redesign of Power System Damping Controllers", IEEE transactions on control systems technology, Vol.-3, No.-3, September-1995.

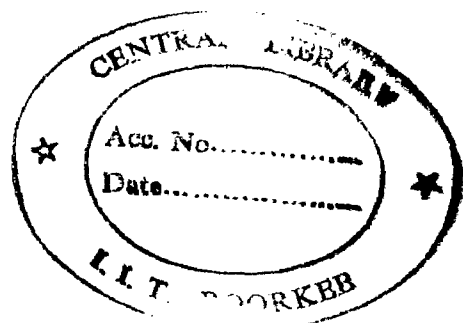
APPENDIX A

BUS DATA OF THE 3-MACHINE, 9-BUS SYSTEM FOR HEAVILY LOADED CONDITION AT BUS NUMBER 5

Bus no.	type	voltage	angle	Load		Generation		Qmin	Qmax
				MW	MVAR	MW	MVAR		
1	1	1.04	0	0	0	0	0	-1	1
2	2	1.025	0	0.0	0	1.63	0	-1	1
3	2	1.025	0	0.0	0	0.85	0	-1	1
4	0	1.0	0	0.0	0	0	0	0	0
5	0	1.0	0	4.9	0.50	0	0	0	0
6	0	1.0	0	0.9	0.3	0	0	0	0
7	0	1.0	0	0.0	0	0	0	0	0
8	0	1.0	0	1.0	0.35	0	0	0	0
9	0	1.0	0	0.0	0	0	0	0	0
10	2	1.015	0	0	0	0	0	-0.8	0.5

BUS DATA OF THE 3-MACHINE, 9-BUS SYSTEM FOR NOMINAL BASE CASE LOADING CONDITION

Bus no.	type	voltage	angle	Load		Generation		Qmin	Qmax
				MW	MVAR	MW	MVAR		
1	1	1.04	0	0	0	0	0	-1	1
2	2	1.025	0	0.0	0	1.63	0	-1	1
3	2	1.025	0	0.0	0	0.85	0	-1	1
4	0	1.0	0	0.0	0	0	0	0	0
5	0	1.0	0	1.25	0.50	0	0	0	0
6	0	1.0	0	0.9	0.3	0	0	0	0
7	0	1.0	0	0.0	0	0	0	0	0
8	0	1.0	0	1.0	0.35	0	0	0	0
9	0	1.0	0	0.0	0	0	0	0	0
10	2	1.015	0	0	0	0	0	-0.8	0.5



LINE DATA OF THE SYSTEM

From	To	R	X	B/2
2	7	0.0	0.0625	0.0
1	4	0.0	0.0576	0.0
3	9	0.0	0.0586	0.0
4	6	0.017	0.092	0.079
4	5	0.01	0.085	0.088
5	10	0.016	0.0805	0.153
10	7	0.016	0.0805	0.153
6	9	0.039	0.17	0.179
9	8	0.0119	0.1008	0.1045
8	7	0.0085	0.072	0.0745

EXCITER DATA

	K_A	T_A
E1	20.0	0.20
E2	20.0	0.20
E3	20.0	0.20

MACHINE DATA

Bus	H	X_d	X_d'	X_q	X_q'	T_{do}	T_{qo}	D
1	23.64	0.1460	0.0608	0.0969	0.0969	8.9600	0.3100	0.0125
2	6.40	0.8958	0.1198	0.8645	0.1969	6.0000	0.5350	0.0068
3	3.01	1.3125	0.1813	1.2578	0.2500	5.8900	0.6000	0.0048

APPENDIX B

LOAD FLOW STUDY
REPORT FOR POWER CALCULATIONS FOR IEEE 10 BUS SYSTEM

LOAD FLOW SOLUTION FOR THE STRESSED OPERATING CONDITION WITHOUT SVC

Bus no	voltage V	angle	Generation		Load		Qmin	Qmax
			MW	MVAR	MW	MVAR		
1	1.0400	0.0000	3.2811	1.6719	0.0000	0.0000	-1.0000	1.0000
2	1.0250	-1.3049	2.2209	0.7543	0.0000	0.0000	-1.0000	1.0000
3	1.0250	-4.0684	1.1455	0.2143	0.0000	0.0000	-1.0000	1.0000
4	0.9647	-10.8580	0.0000	0.0000	0.0000	0.0000	0.0000	0.0000
5	0.8671	-27.3287	-0.0000	0.0000	4.5000	0.5000	0.0000	0.0000
6	0.9649	-12.9260	-0.0000	0.0000	0.9000	0.3000	0.0000	0.0000
7	0.9883	-9.1804	-0.0000	0.0000	0.0000	0.0000	0.0000	0.0000
8	0.9859	-10.9753	-0.0000	0.0000	1.0000	0.3500	0.0000	0.0000
9	1.0149	-7.7681	-0.0000	0.0000	0.0000	0.0000	0.0000	0.0000
10	0.9218	-17.7272	-0.0000	0.0000	0.0000	0.0000	0.0000	0.0000

LOAD FLOW STUDY
REPORT FOR POWER CALCULATIONS FOR IEEE 10 BUS SYSTEM

LOAD FLOW SOLUTION FOR STRESSED CASE OPERATING CONDITION WITH SVC

Bus no	type	voltage V	Angle	Generation		Load		Qmin	Qmax	
				MW	MVAR	MW	MVAR			
1	1	1.0400	0.0000	3.3241	1.3683	0.0000	0.0000	-1.3683	-1.0000	1.0000
2	2	1.0250	-2.3869	2.1755	0.3965	0.0000	0.0000	-0.3965	-1.0000	1.0000
3	2	1.0250	-4.6683	1.1227	0.0843	0.0000	0.0000	-0.0843	-1.0000	1.0000
4	0	0.9816	-10.8096	-0.0000	0.0000	0.0000	0.0000	-0.0000	0.0000	0.0000
5	0	0.9089	-26.4406	0.0000	0.0000	4.5000	0.5000	0.0000	0.0000	0.0000
6	0	0.9795	-13.0007	-0.0000	0.0000	0.9000	0.3000	-0.0000	0.0000	0.0000
7	0	1.0096	-9.9369	-0.0000	0.0000	0.0000	0.0000	-0.0000	0.0000	0.0000
8	0	1.0018	-11.5569	-0.0000	0.0000	1.0000	0.3500	-0.0000	0.0000	0.0000
9	0	1.0222	-8.2684	-0.0000	0.0000	0.0000	0.0000	-0.0000	0.0000	0.0000
10	2	0.9760	-18.0723	-0.0000	0.5000	0.0000	0.0000	-0.5000	-0.5000	0.5000

Type : 1 swing bus
2 PV bus
3 PQ bus

SVC installed at 10th bus
Line power flow $P_{10-7} = 1.7982 + 0.5100j$

LOAD FLOW STUDY
REPORT FOR POWER CALCULATIONS FOR IEEE 10 BUS SYSTEM

LOAD FLOW SOLUTION FOR THE BASE OPERATING CONDITION OF POWER SYSTEM WITHOUT SVC

Bus no	type	Voltage V	Angle	Generation		Load		Qmin	Qmax
				MW	MVAR	MW	MVAR		
1	1	1.0400	0.0000	0.7163	0.2688	0.0000	0.0000	-1.0000	1.0000
2	2	1.0250	9.2499	1.6300	0.0664	0.0000	0.0000	-1.0000	1.0000
3	2	1.0250	4.6470	0.8500	-0.1089	0.0000	0.0000	-1.0000	1.0000
4	0	1.0259	-2.2163	0.0000	0.0000	0.0000	0.0000	0.0000	0.0000
5	0	0.9959	-3.9822	-0.0000	0.0000	1.2500	0.5000	0.0000	0.0000
6	0	1.0127	-3.6930	-0.0000	0.0000	0.9000	0.3000	0.0000	0.0000
7	0	1.0258	3.6897	-0.0000	0.0000	0.0000	0.0000	0.0000	0.0000
8	0	1.0159	0.7027	0.0000	-0.0000	1.0000	0.3500	0.0000	0.0000
9	0	1.0324	1.9490	-0.0000	0.0000	0.0000	0.0000	0.0000	0.0000
10	0	1.0148	-0.1600	0.0000	-0.0000	0.0000	0.0000	0.0000	0.0000

LOAD FLOW STUDY
REPORT FOR POWER CALCULATIONS FOR IEEE 10 BUS SYSTEM

LOAD FLOW SOLUTION FOR THE BASE OPERATING CONDITION OF POWER SYSTEM WITH SVC

Bus no	type	Voltage V	Angle	Generation		Load		Qmin	Qmax
				MW	MVAR	MW	MVAR		
1	1	1.0400	0.0000	0.7163	0.2679	0.0000	0.0000	-1.0000	1.0000
2	2	1.0250	9.2483	1.6300	0.0652	0.0000	0.0000	-1.0000	1.0000
3	2	1.0250	4.6466	0.8500	-0.1093	0.0000	0.0000	-1.0000	1.0000
4	0	1.0259	-2.2161	-0.0000	0.0000	0.0000	0.0000	0.0000	0.0000
5	0	0.9960	-3.9820	-0.0000	0.0000	1.2500	0.5000	0.0000	0.0000
6	0	1.0128	-3.6928	-0.0000	0.0000	0.9000	0.3000	0.0000	0.0000
7	0	1.0259	3.6884	-0.0000	0.0000	0.0000	0.0000	0.0000	0.0000
8	0	1.0160	0.7021	0.0000	-0.0000	1.0000	0.3500	0.0000	0.0000
9	0	1.0324	1.9487	-0.0000	0.0000	0.0000	0.0000	0.0000	0.0000
10	2	1.0150	-0.1617	0.0000	0.0023	0.0000	0.0000	-0.5000	0.5000

Type : 1 swing bus

2 PV bus

3 PQ bus

SVC installed at 10th bus

line power flow $P_{10-7} = 0.8675 - 0.0839j$